Annual Technical Progress Report
(Oct. 1, 2002 – Sept. 30, 2003)

DEVELOPMENT AND OPTIMIZATION OF GAS-ASSISTED GRAVITY DRAINAGE (GAGD) PROCESS FOR IMPROVED LIGHT OIL RECOVERY

Work Performed Under Cooperative Agreement
DE-FC26-02NT15323

By

Dandina N. Rao, Ph. D., P. Eng.
(Principal Investigator)

Qiang Xu, Ph. D.
(Research Associate)
Subhash C. Ayirala, M. S.
Madhav M. Kulkarni, M. S.
Amit P. Sharma, M. S.
(Graduate Research Assistants)

The Craft & Hawkins Department of Petroleum Engineering
Louisiana State University
Baton Rouge, LA 70803

October 2003

Prepared for
U. S. Department of Energy
National Petroleum Technology Office

DISCLAIMER

Annual Technical Progress Report
(Oct. 1, 2002 – Sept. 30, 2003)

DEVELOPMENT AND OPTIMIZATION OF GAS-ASSISTED GRAVITY DRAINAGE (GAGD) PROCESS FOR IMPROVED LIGHT OIL RECOVERY

Work Performed Under Cooperative Agreement
DE-FC26-02NT15323

By

Dandina N. Rao, Ph. D., P. Eng.
(Principal Investigator)

Qiang Xu, Ph. D.
(Research Associate)
Subhash C. Ayirala, M. S.
Madhav M. Kulkarni, M. S.
Amit P. Sharma, M. S.
(Graduate Research Assistants)

The Craft & Hawkins Department of Petroleum Engineering
Louisiana State University
Baton Rouge, LA 70803

October 2003

Prepared for
U. S. Department of Energy
National Petroleum Technology Office

Abstract

This is the first Annual Technical Progress Report being submitted to the U. S. Department of Energy on the work performed under the Cooperative Agreement DE-FC26-02NT15323. This report follows two other progress reports submitted to U. S. -DOE during the first year of the project: The first in April 2003 for the project period from October 1, 2002 to March 31, 2003, and the second in July 2003 for the period April 1, 2003 to June 30, 2003. Although the present Annual Report covers the first year of the project from October 1, 2002 to September 30, 2003, its contents reflect mainly the work performed in the last quarter (July – September, 2003) since the work performed during the first three quarters has been reported in detail in the two earlier reports.

The main objective of the project is to develop a new gas-injection enhanced oil recovery process to recover the oil trapped in reservoirs subsequent to primary and/or secondary recovery operations. The project is divided into three main tasks. Task 1 involves the design and development of a scaled physical model. Task 2 consists of further development of the vanishing interfacial tension (VIT) technique for miscibility determination. Task 3 involves the determination of multiphase displacement characteristics in reservoir rocks. Each technical progress report, including this one, reports on the progress made in each of these tasks during the reporting period.

Section I covers the scaled physical model study. A survey of literature in related areas has been conducted. Test apparatus has been under construction throughout the reporting period. A bead-pack visual model, liquid injection system, and an image analysis system have been completed and used for preliminary experiments. Experimental runs with decane and paraffin oil have been conducted in the bead pack model. The results indicate the need for modifications in the apparatus, which are currently underway. A bundle of capillary tube model has been considered and formulated aiming to reveal the interplay of the viscous, interfacial and gravity forces and to predict the gravity drainage performance. Scaling criteria for the scaled physical model design have been proposed based on an inspectional analysis.

In Section II, equation of state (EOS) calculations were extended to study the effect of different tuning parameters on MMP for two reservoir crude oils of Rainbow Keg River and Terra Nova. This study indicates that tuning of EOS may not always be advisable for miscibility determination. Comparison of IFT measurements for benzene in water, ethanol mixtures with the solubility data from the literature showed that a strong mutual relationship between these two thermodynamic properties exists. These preliminary experiments indicate applicability of the new vanishing interfacial tension (VIT) technique to determine miscibility of ternary liquid systems. The VIT experimental apparatus is under construction with considerations of expanded capacity of using equilibrated fluids and a new provision for low IFT measurement in gas-oil systems.

In Section III, recommendations in the previous progress reports have been investigated in this reporting period. WAG coreflood experiments suggest the use of 'Hybrid'-WAG type floods for improved CO_2 utilization factors and recoveries. The effect of saturating the injection water with CO_2 for corefloods has been investigated further in this quarter. Miscible WAG floods using CO_2 saturated brine showed higher recoveries (89.2% ROIP) compared to miscible WAG floods using normal brine (72.5%). Higher tertiary recovery factors (TRF) were also observed for WAG floods using CO_2 saturated brine due to improved mobility ratio and availability of CO_2. Continued experimentation for evaluation of both, 'Hybrid'-WAG and gravity stable type displacements, in Berea sandstone cores using synthetic as well as real reservoir fluids are planned for the next quarter.

Table of Contents

I. DESIGN AND DEVELOPMENT OF A SCALED EXPERIMENTAL GAGD MODEL 1

1.1. Summary of previous work 1

1.2. Introduction to work in the latest quarter - A petrophysical study on gravity drainage process in porous media 1

1.3. The gravity drainage experiment 2

1.4. Petrophysical analysis 7

1.5. A bundle of capillary model for 1-D gravity drainage 9

1.6. An inspectional analysis of gravity drainage process. 12

1.7. Additional gravity drainage experiments 17
- 1.7.1 Scaled Physical Model of Gas-Assisted Gravity Drainage 17
- 1.7.2 Experimental Strategies, Procedure, Results and Discussion 19

II. FURTHER DEVELOPMENT OF THE VANISHING INTERFACIAL TENSION (VIT) TECHNIQUE 31

2.1 Comparison of Gas/Oil IFT Measurements with Parachor Model 31
- 2.1.1 Introduction 31
- 2.1.2 Objective 32
- 2.1.3 Methodology 33
- 2.1.4 Results and Discussion 33

2.2 Effect of GOR on IFTs Determined from Parachor Model 33
- 2.2.1 Results and Discussion 33

2.3 Comparison of VIT MMPs with EOS Calculations and Parachor Models 34
- 2.3.1 MMP Determination using EOS 34
- 2.3.2 MMP calculation using Parachor Computational Model 35
- 2.3.3 Results and Discussion 35

2.4 IFT Measurements of a Standard Ternary Liquid System 36
2.4.1 Capillary Rise Technique 36

2.5 Conclusions 37
2.5.1 Comparison of Gas/Oil IFT Measurements with Parachor Model 37
2.5.2 Effect of GOR on IFTs Determined from Parachor Computational Model 37
2.5.3 Comparison of VIT MMPs with EOS Calculations and Parachor Models 38
2.5.4 IFT Measurements of a Standard Ternary Liquid System 38

2.6 Future Plans 38

III. DETERMINATION OF MULTIPHASE DISPLACEMENT CHARACTERISTICS IN RESERVOIR ROCKS 43

3.1 Abstract 43

3.2 Research Focus 44

3.3 Literature Review 45
3.3.1 Summary of Laboratory and Theoretical Studies 45
3.3.2 Summary of Field Applications 46

3.4 Experimental Design 47

3.5 Coreflood Results 49
3.5.1 Determination of Solubility of CO_2 in Yates Reservoir Brine 49
3.5.2 Miscible WAG Flood In Berea Rock, CO_2-Saturated Yates Brine, and n-Decane System 51

3.6 Status and Future Work 55
3.6.1 Status 55
3.6.2 Future Work 56

Appendix 1. Literature Review a1

I. Design and Development of a Scaled Experimental GAGD Model

1.1. Summary of previous work

Progress on Task 1 prior to this quarter has been reported in previous quarterly reports (15323R01 and 15323R02). In those reports, a thorough survey of literature in related areas has been reported. A bead-pack visual model, liquid injection system, and an image analysis system have been set up, and used for preliminary experiments. Three experimental runs have been conducted with decane, water, and air system in a beadpack. Experimental results illustrate the importance of gravity segregation in the displacement process. During the free gravity drainage of decane, air encroachment was observed, and the phenomenon may be important in oil gravity drainage during gravity-stable gas injection in reservoirs.

1.2. Introduction to work in the latest quarter - A petrophysical study on gravity drainage process in porous media

The gravity drainage mechanism is important in the development of many oil reservoirs with large dipping angle or significant vertical thickness and permeability. This mechanism is also important in ground water infiltration. Both in laboratory and in many field applications, it has been found that high oil recoveries can be achieved by applying of gravity drainage process. For example, Kantzas et al. (1988) reported gravity drainage laboratory experimental results using unconsolidated media with maximum oil recovery of 99% of the initial oil in place (IOIP). DesBrisay et al. (1981) reported a projected ultimate recovery of 70% IOIP in Intisar 'D' field. Da Sle and Guo (1990) reported a projected ultimate recovery of 94% IOIP in Westpem Nisku D Reef field.

Characterizing and modeling the gravity drainage process theoretically are still a great challenge, however. Several gravity drainage models have been developed and reported in the literature (Cardwell and Parsons, 1948; Hagoort, 1980; Ypma, 1985; Luan, 1994). However, these models are far from solving the problem due to the complexity of the gravity drainage process.

Lack of predictive theoretical approach, laboratory experiments may be a way to predict gravity drainage performance. To properly scale up the laboratory data to the field scale, the laboratory physical model should be similar to the specific reservoir in geometry, physical processes, and even chemical processes. To build such a similar system, one needs good understanding of the process and interplays of the physical forces. In this article, we introduce detailed gravity drainage experimental results and discuss the interplays of the gravity, capillary and viscous forces in the case. Based on experimental observations, a preliminary bundle of capillary tube model aiming to gain a better understand of the process was proposed. Finally, an inspectional analysis on 1-D gravity drainage is carried out and subsequent scaling criteria that a laboratory model should obey are proposed. More experimental results are included in Section 1.7.

1.3. The gravity drainage experiment

Experimental conditions: this experiment was conducted in the following steps (for detailed experimental setups, see Rao et al., 2003):

- Imbibe deaerated water into the pack from the bottom at a sufficiently large hydraulic head to ensure near full saturation in the pack with water; record volume imbibed.
- Displace water with oil (paraffin) downward (i. e. gravity stable mode) at a constant injection rate until oil breaks through and no water is produced; record produced volume of oil.
- Open top and bottom of the pack to atmosphere; let gravity drainage occur at the free air inflow condition; collect effluent in a glass cylinder. Measure the volumetric increase of oil and water in the glass cylinder; Measure also the rate of advance of the air/oil interface in the bead pack.

Initial pack condition prior to gravity drainage: in the first step, a total of 534 cc of water was imbibed into the pack. During the oil displacement step, 520 cc of oil was injected and 30 cc of oil was produced, giving an initial oil in place (IOIP) of 490 cc. Initial water in place was therefore 44 cc (S_{cw} = 0.082). In system where oil/gas/water phases coexist, fluids distribution and thus their flow properties depend on interactions between rock and fluids, such as interfacial tension, wetting, and saturation history. Previous studies (*e.g.* Vizika and Lombard, 1996) showed that wettability and spreading coefficient are important in the process. In this study, we have used a water-wet and a ternary fluids (paraffin/air/water) system, which was a positive spreading system. Connate water is assumed to occupy the smallest pore spaces, and to coat on solid grains, and to be immobile during the gravity drainage process. Oil is assumed to spread on water forming a continuous film in the gas invaded zone in accordance with the positive spreading coefficient of the fluid system used in the test.

Experimental results: as shown in Figures 1.1(a) to 1.1(g), a clear-cut air/oil interface between the gas zone and oil bank can be observed. Slight gas invasion in the oil bank is visible in Figure 1.1 as indicated by the lighter color in upper portion of the oil bank. The light color pattern in oil bank as indicated in the circle is taints inside the Pyrex glass plate, noticing that the pattern remains unchanged. Leave-behind oil in gas zone is more evident as indicated by the dark dots. The leave-behind oil saturation can also be inferred from material balance. Oil drainage ceased at the time in Figure 1.1(g) due to the capillary end effect. During the process, no water was produced, supporting the assumption that the water (at its initial saturation of 0.082) is immobile during gravity drainage.

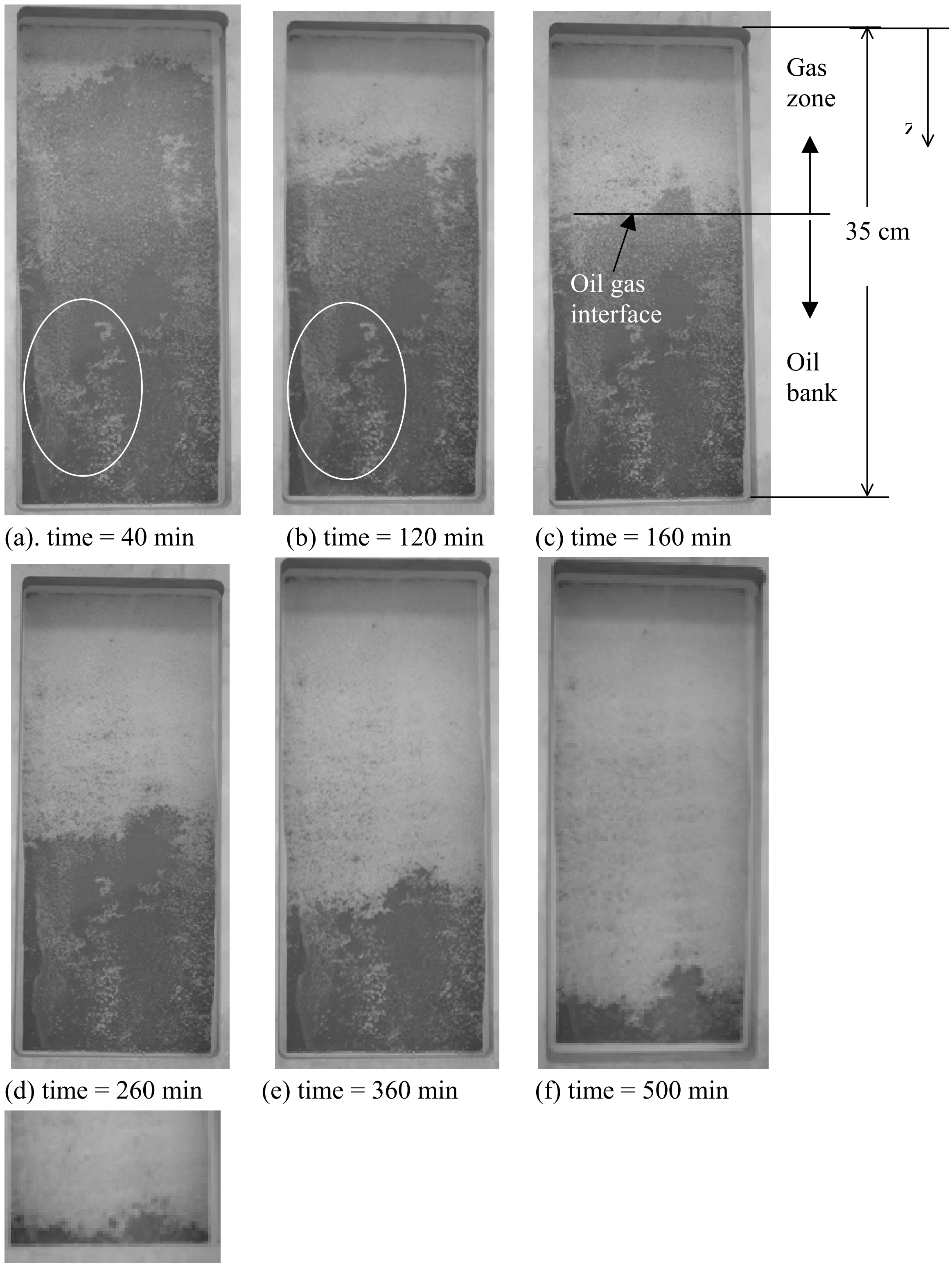

(a). time = 40 min (b) time = 120 min (c) time = 160 min

(d) time = 260 min (e) time = 360 min (f) time = 500 min

(g) time = 540 min

Figure 1.1. Oil/air interface advances in bead pack under free gravity drainage.

Figure 1.2(a) shows cumulative oil recovery versus time. As gas initially broke through from the outlet at "A" (corresponding to Figure 1.1(g)), both oil and gas flow ceased thereafter until point "B", where oil started flow again due to the formation of a secondary oil bank from the film drainage flow in the gas zone. Our interest in this section is on the linear regime shown in Figure 1.2(b), which shows that the oil production indeed is linear to time before 400 minute.

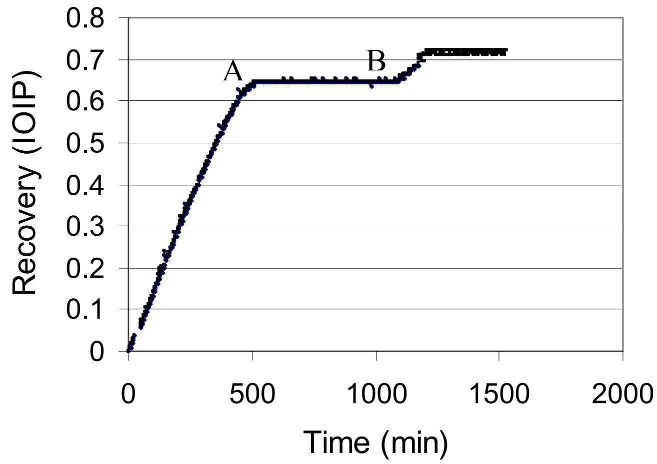

Figure 1.2(a). Oil recovery (in fraction of the IOIP) in free gravity drainage experiment.

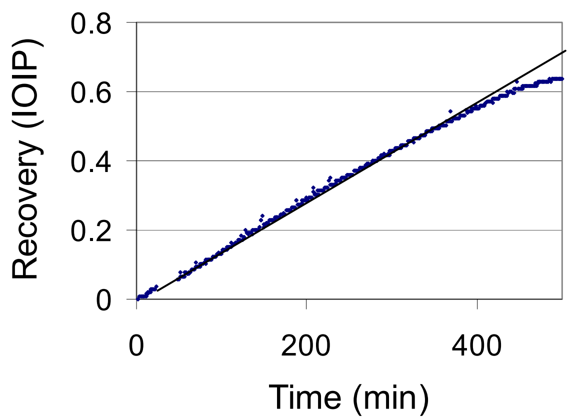

Figure 1.2(b). Oil recovery in free gravity drainage experiment before air break through.

Figures 1.3 and 1.4, plotted in the same time scale with Figure 1.2, show gas zone expansion and the calculated average gas saturation in the oil bank. The dimensionless gas zone length in Figure 1.3 is defined as the fraction of the gas zone length to the height of the pack.

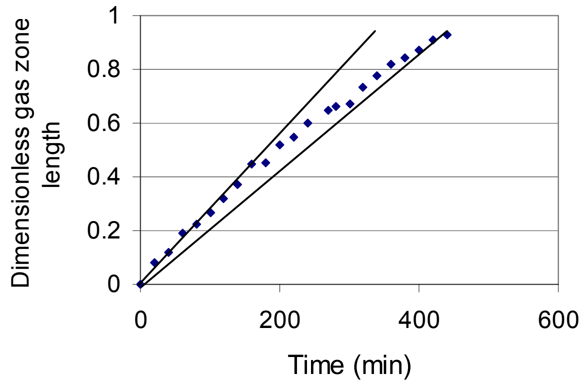

Figure 1.3. Gas zone expansion over time (vertical axis is the fraction of gas zone length to the total length of the bead pack).

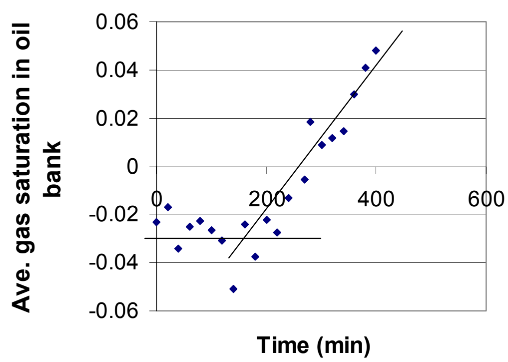

Figure 1.4. Calculated average gas saturation in oil bank.

Corresponding to the constant rate oil production, the gas inflow rate must be constant since there can be no pressure change during the free-fall gravity drainage experiment within the gas zone. However, Figure 1.3 shows that the downward gas zone expansion rate decreases gradually over time (this is also reported in Grattoni et al. (2001)), meaning that there is increased amount of gas invasion into the oil bank if we assume average leave-behind oil saturation in gas zone does not change. This assumption maybe justified with the following arguments. The oil film drainage is a slow process, in which the oil saturation in the lower part in the pack (larger z in Figure 1.1) increases while it decreases in the upper part (smaller z in Figure 1.1). The oil saturation in gas zone above the interface is lower than that at the top of the oil bank, thus the saturation wave moves at a slower velocity than the air-oil interface. Therefore, the leave-behind oil remains in the gas zone in the process before (g), where oil ceases flow at the outlet. The average leave-behind oil saturation in the gas zone can be determined at this point with material balance to be 0.35 IOIP.

With the average oil saturation in the gas zone determined, we can also calculate average gas saturation in the oil bank by material balance. The volume of gas in oil bank combined with the oil in the oil bank, which is the total volume of oil initially present in the pack minus the produced and leave-behind oil, makes up the volume of the oil bank. As shown in Figure 1.4, the average gas saturation increases from 200 minutes to 400 minutes as expected; whereas average gas saturation is negative in the early time. The latter may reflect experimental artifacts, like inexactness of measurements and the initial dead volume at top of the pack.

Without a reliable technique for local saturation measurements, it is difficult to obtain a quantitative saturation profile. However, a qualitative gas saturation profile (Figure 1.5) can be inferred from the experimental results. This is analogous to saturation profile in the Buckley-Leverett displacement. However, the physical nature of this process may not be the same as in a forced immiscible displacement. We discuss the physical forces in more details below.

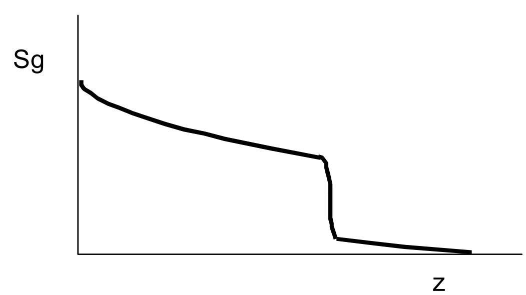

Figure 1.5. Schematic of gas saturation profile in bead pack.

1.4. Petrophysical analysis

- Near single phase oil flow in the oil bank
- The capillary, viscous and gravitational forces at the oil/gas interface
- Two-phase oil/gas flow in gas zone.

In this particular case, gas invasion into the oil bank appears to be insignificant. In addition, the gas invasion rate was slow and gas-break through was not observed. Therefore, the oil in the lower portion of the oil bank was flowing nearly in a single-phase flow mode at constant driving force or pressure gradient, the gravitational force $\Delta\rho g$. The Darcy's law applies in the single-phase oil flow region, and constant production rate was confirmed in the experiment. The decrease in oil rate during the later time (see

Figure 1.3) likely is a result of increase of gas invasion, decreases of oil saturation, and thus its relative permeability.

The invasion of gas into the oil bank did not affect the production behavior in any significant degree in this case. However, gas invasion can be significant should the oil were more viscous and pore-throat size distribution was more scattered towards larger size.

The invasion of gas in the oil bank distinguishes this process from a forced displacement, where the displacing phase saturation in front of shock is zero (or constant if present initially) theoretically (Buckley and Leverett, 1941; Lake, 1989). Capillary force does smear the shock front, but doesn't lead to continuous spreading-out of the shock front. The Buckley-Leverett shock can be quite sharp in large scale. The physical reason for the formation of shock is the self-sharpening mechanism, saturation wave velocity at lower displacing phase saturation moves slower, higher saturation behind catches up, thus no lower saturation can present in front of the shock. In the gravity drainage, the phase original in place is driven away by the gravitational force rather than the displacing phase, and the gas phase merely fill-up the voids left behind.

The original phase drains preferably in the relative larger channels. The voids left-behind are open to adjacent liquid and gas, both has a tendency to occupy the void space. Let us use Figure 1.6 to illustrate the scenario. Assume the oil in the lower pore drains down and empties the pore, the adjacent fluids in the liquid filled and gas filled pores both has the tendency to fill-up this void. The liquid drainage is driven by gravitational force and the gas by pressure (in the free fall gravity drainage process, this pressure is the atmospherically pressure). This competition results in likely both phases present in the lower pore in a proportion that depends on the velocity of the liquid flow, mobilities and densities of the phases (if gas can overcome the capillary pressure in the pore throat that connects the gas filled pore and the lower pore). The faster the velocity of the fluids, the higher is the resistance to the liquid flow, thus the higher is the left-behind of the liquid phase. This is a different effect of velocity to that in a displacement. With capillary and gravity forces playing the same role, the viscous force, normally expressed as $v\mu$ (v is the superficial velocity, μ is viscosity of the displacing phase) may not have the same role in a gravity drainage process as in a displace process.

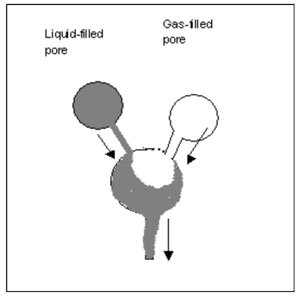

Figure 1.6. Schematic of a simplified pore structure and phase distribution

Of course, such a simple conjecture cannot be sufficient to explain what happens in the process. A network model (Bryant and Blunt, 1992), which is out of the scope of this study, with realistic pore structure and realistic model for microscopic fluid distribution (wetting) and flow could be an approach to solve this problem. Nevertheless, the simply conjecture does show that gravity drainage is distinctive from an immscible displacement.

In the gas zone, oil is hydraulically continuous due to the spreading condition. The oil flows as films with a typical relative permeability in the order of S_o^2 (Dicarlo et al., 2000). The gas is almost stagnant, with insignificant transverse flow as well. Gas phase is also continuous.

1.5. A bundle of capillary model for 1-D gravity drainage

Fluid flow behavior in porous media can be explained by considering that the porous solid behaves as a simple bundle of capillaries of different radii (Nutt, 1982). In a gravity drainage process, flow is in one dimension downward in the gravity stable mode, making it more appropriate to use the bundle of capillary tube model. Vertical capillary tube with varying radii R_i is the basic building block in this model, a series of such tubes in the same length but with different radii is used to represent pore throats that transport fluid in a porous medium. There is no cross flow or communication among these tubes. Therefore, analyze flow in one capillary tube and integrate the results over the full range of the radii provides an approach to reach a solution for this process.

Flow in the capillary tube. Steady-state laminar flow is assumed within a capillary tube as show in Figure 1.7.

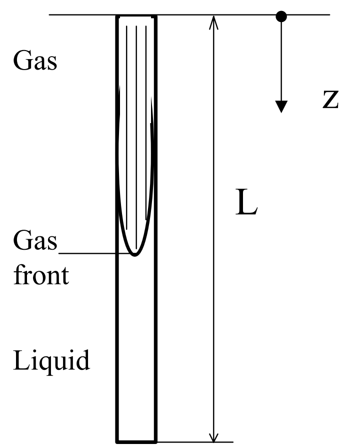

Figure 1.7. A capillary tube and fluid distribution.

The shape of the interface is assumed depending on the liquid flow profile, not the capillary pressure before capillary equilibrium is reached. Solution for such a Newtonian flow in cylindrical tube is available in Bird et al. (1960). The velocity profile in the vertical cross section as a function of the distance from the center is,

$$u_{rz} = [\Delta\mathscr{P} R_i^2/(4\mu(L-z)][1-(r/R_i)^2] \qquad (1.1)$$

where u_{rz} is the velocity in z direction; $\Delta\mathscr{P} = (\rho g\Delta z + \Delta p)$ is the potential difference and Δp is applied pressure over the distance of (L-Z), μ is the oil viscosity, r is the distance from the center of the tube. With this flow equation, we can calculate "oil saturation, S_o" at anytime at any position in the tube. From Eq. 1.1, we have,

$$\pi(R_i^2-r^2) = (4\mu(L-z)z)/ (\Delta\mathscr{P} t) \qquad (1.2)$$

this gives the annulus area that is still occupied by liquid. At r = 0, gas front just arrive to position z, we have

$$R' = (4\mu(L-z)z)/ (\Delta\mathscr{P} t)^{1/2} \qquad (1.3)$$

This gives the $R_i = R'$ where gas front just arrives, for any $R_i > R'$, the portion that still occupied by oil can be calculated using Eq. 1.2, for any $R_i \leq R'$, gas not yet arrived and the cross section of that tube is oil filled. Combining the saturation for all the tubes gives the saturation at the position at that time in the media,

$$So(z,t) = \left[\int_{R'}^{R_1} \gamma(R_i)\, 4\mu(L-z)z / (\Delta\mathcal{P}t) dR_i + \int_{R'}^{R_1} \pi R_i^2 \gamma(R_i) dR_i \right] / \int_{R_0}^{R_1} \pi R_i^2 \gamma(R_i) dR_i \qquad (1.4)$$

where $\gamma(R_i)$ is the density distribution function, which specifies the probability of a capillary tube who's radii to be a particular value. The form of this function depends on the pore throat size distribution, which may be obtained from imaging technology (Bakke and Oren, 1997) or the traditional mercury test. The average saturation strongly depends on the density distribution function $\gamma(R_i)$. With the density function determined, a solution for saturation profile and thus the production rate and cumulated production of oil can be obtained.

Capillary pressure. The drive force for the flow is the gravitational force, and the flow is hindered by capillary pressure acting like a negative pressure upwards at the phase interface, contributing to the potential term in Eq. 1.1. Capillary pressure in a tube of radius of R_i is:

$$P_c = (2\sigma\cos\theta)/R_i \qquad (1.5)$$

where σ is the interfacial tension and θ is the contact angle. Capillary pressure that acts at the gas/oil interface is a constant in a particular tube, it slows down the flow as the length of the liquid reduces because the pressure gradient implied by capillary force increases, whereas the gravitational gradient is a constant. When the capillary force and gravitational force becomes equal to each other or at capillary equilibrium,

$$P_c = \Delta\rho g(L-z) \qquad (1.6)$$

the flow stops. This represents the well-known capillary end-effect, the accumulation of wetting phase at the end of cores. The height of liquid column at which flow stops can be determined by Eq. 1.6 for a giving capillary tube. Similarly, residual liquid saturation in the porous media caused by the capillary end-effect can be determined by integration over the range of all tubes.

Although a simple model, bundle of capillary tube model captures some important physical insides and tells us what the capillary force and gravitational force does in the process. This model also illustrates the importance of pore throat size distribution function, which should always be considered in a scale up from a different porous medium.

1.6. An inspectional analysis of gravity drainage process.

Gravity drainage process is difficult to model theoretically. Here we use an inspectional analysis approach that presents the governing equations, derive their dimensionless forms, and combine variables into dimensionless groups. Similarity groups are then proposed based on these dimensionless groups and other considerations as well.

To begin this derivation, the following assumptions are made,

- One-dimensional downward flow.
- Isothermal condition.
- Immiscible gas/oil phases.
- Incompressible phases and porous media.
  The pressure in this process is not expected to vary in any significant way. Therefore, it is still reasonable to assume incompressible phases.
- Spreading system,
  $K = \sigma_{wg} - (\sigma_{og} + \sigma_{ow}) > 0$,
  Where K is the spreading coefficient, and σ is the interfacial tension between the phases. When K is positive, oil spreads on water.
- Water-wet media, water occupies smallest pores and coats grain particles, water is immobile throughout the process.
- Three-phase co-existence, but can be simplified as an oil/gas two phase flow problem by assuming connate water saturation for oil water system is the same for gas water system.

The analysis. The problem is reduced to an oil/gas two-phase flow problem under the above assumptions. As show in Figure 1.8, we have constant production rate at u, which is equal to the sum of u_1 (oil) and u_2(gas). There are two regions in the column, one is the oil bank at connate water saturation, and the other is the gas-invaded zone.

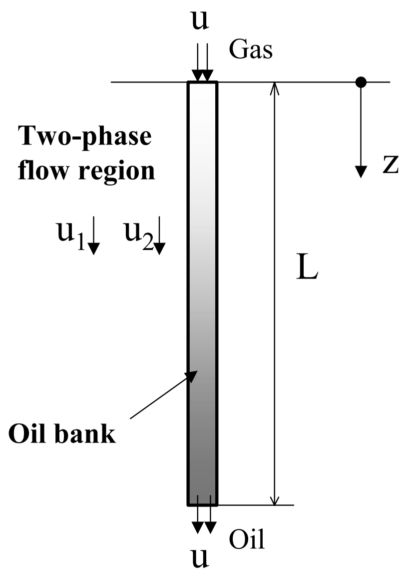

Figure 1.8. Schematic of the 1-D gravity drainage in porous media

The mass conservation equation:

$$\phi \frac{\partial S_1}{\partial t} + \frac{\partial u_1}{\partial z} = 0 \quad (1.7)$$

where subscript "1" refers the oil phase.

The flow equation is Darcy's law applied to the oil and gas phases:

$$u_1 = kk_{r1} / \mu_1 (\frac{dp_1}{dz} + \rho_1 g) \quad (1.8)$$

$$u_2 = kk_{r2} / \mu_2 (\frac{dp_2}{dz} + \rho_2 g) \quad (1.9)$$

where k is the absolute permeability; k_r is relative permeability; μ and ρ are viscosity and density of the phases respectively.

From the incompressible assumption and capillary relation, we have

$$u_1 + u_2 = u \quad (1.10)$$

$$p_2 = p_1 + p_c \quad \text{(1.11)}$$

where

$$p_c = \sigma\sqrt{\frac{\phi}{k}}J(S_1) \quad \text{(1.12)}$$

$J(S_1)$ is the dimensionless capillary pressure, Leverett J function, and σ is the interfacial tension.

The initial and boundary conditions are:

$$S_1 = S_{1i} \qquad at \quad t = 0, \quad 0 \le z \le L$$

$$u_1 = 0 \qquad at \quad t > 0, \qquad z = 0$$

$$u_2 = 0 \qquad at \quad t < t_{BT}, \qquad z = L \quad \text{(1.13)}$$

where t_{BT} is the gas breakthrough time.

Now we transform the equations to their dimensionless forms by applying the following transformation.

$$\begin{aligned}
z_D &= x / L \\
t_D &= t / t^* \\
u_{1D} &= u_1 / u \\
u_{2D} &= u_2 / u \\
p_{1D} &= p_1 /(\sigma\sqrt{\frac{\phi}{k}}) \\
p_{2D} &= p_2 /(\sigma\sqrt{\frac{\phi}{k}}) \\
J(S_1) &= p_c /(\sigma\sqrt{\frac{\phi}{k}})
\end{aligned} \quad \text{(1.14)}$$

where t* is to be determined.

Substitute Eq. 1.14 into Eqs. 1.7-1.13, we get the following dimensionless form of the equations:

$$\frac{\partial S_1}{\partial t_D} + \frac{\partial u_{1D}}{\partial z_D} = 0 \ldots\ldots\ldots\ldots\ldots\ldots\ldots\ldots\ldots\ldots\ldots\ldots\ldots\ldots\ldots\ldots\ldots\ldots\ldots\ldots (1.7')$$

$$u_{1D} = k_{r1}(D_1 \frac{dp_{1D}}{dz_D} + D_2) \ldots\ldots\ldots\ldots\ldots\ldots\ldots\ldots\ldots\ldots\ldots\ldots\ldots\ldots\ldots\ldots (1.8')$$

$$u_{2D} = k_{r2}(D_3 \frac{dp_{2D}}{dz_D} + D_4) \ldots\ldots\ldots\ldots\ldots\ldots\ldots\ldots\ldots\ldots\ldots\ldots\ldots\ldots\ldots\ldots (1.9')$$

In Eqs. 1.7'-1.13', we have

$$t^* = \frac{\phi L}{u}$$

$$D_1 = \frac{k\sigma}{L\mu_1 u}\sqrt{\frac{\phi}{k}}$$

$$D_2 = \frac{\rho_1 g k}{\mu_1 u}$$

$$D_3 = \frac{k\sigma}{L\mu_2 u}\sqrt{\frac{\phi}{k}}$$

$$D_4 = \frac{\rho_2 g k}{\mu_2 u}$$

These dimensionless groups are not unique to the problem, other combinations may have better physical meanings. Let us define $D_5 = D_2/D_4 = \rho_1/\rho_2$, then we can delete D4 from the groups. Similarly, by defining $D_6 = D_1/D_3 = \mu_2/\mu_1$, we can delete D_1 from the groups; and D_7 such that $D_6\, D_7 = D_2/D_3$, then $D_7 = \dfrac{\rho_1 g L}{\sigma\sqrt{\frac{\phi}{k}}}$. Finally, our similarity groups after these transformations are:

$$\frac{\rho_1}{\rho_2}, \frac{\mu_2}{\mu_1}, \frac{\rho_1 g k}{\mu_1 u}, \frac{\rho_1 g L}{\sigma\sqrt{\frac{\phi}{k}}},$$

groups 1 and 2 are density and viscosity ratios; group 3 is the ratio of gravity to the viscous forces, or a gravity number; and group 4 is the ratio of gravity force to capillary forces, which is the Bond number. The reason for these transformations is that the gravitational force is considered the most important among the viscous, capillary and gravitational forces in the drainage process being considered.

The dimensionless relative permeability terms of oil and gas appear in Eqs. 1.8' and 1.9'. The initial condition in Eq. 1.13 provides yet another dimensionless group, S_{1i}, the initial oil saturation. To ensure the same relative permeability function in the model and in the field, it is ideal to use the same reservoir rock material in the physical model. However, this is not always possible. If different porous media are used, the pore size distribution should be matched in the prototype and the physical model. In other words, the pore size distribution functions should be congruent functions as shown in Figure 1.9.

To ensure the same initial saturation condition, let us use Figure 1.9 to illustrate the point.

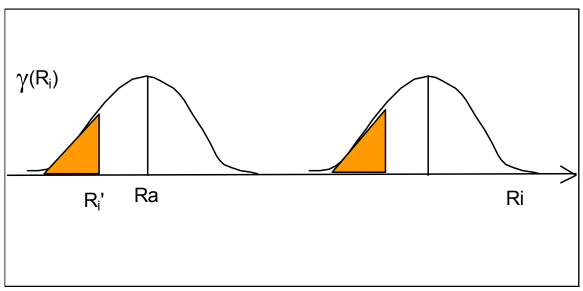

Figure 1.9. Congruent pore throat size distribution functions

Same saturation in the model as in the field means that the same proportion of space is occupied by the wetting phase with the same distribution function, represented by the dark-colored area. The entry pore throat size, R_i' that is determined by capillary pressure, should correspond to each other in terms of their relative magnitude, that is R_i'/R_a should be the same for the model and field, where R_a can be the average pore throat size.

The initial drainage process in the oil reservoir is a capillary and gravity dominated process, i. e., oil migrate due to force and enters pores with a certain pore throat opening depending on the capillary pressure. The capillary pressure should be equal to the gravity force that drives water away. So,

$$P_c = 2\sigma\cos\theta/R_i'$$

$$R_i' = 2\sigma\cos\theta / P_c \quad \ldots\ldots\ldots\ldots\ldots\ldots\ldots\ldots\ldots\ldots\ldots\ldots\ldots\ldots\ldots\ldots\ldots\ldots\ldots (1.10)$$

Where capillary pressure P_c was balanced by the gravity force. Thus the value of P_c can be determined by the oil-water contact and density difference of oil and water in a specific reservoir. This quantity can be transformed by dividing it with the average pore throat radius R_a, gives:

$$2\sigma\cos\theta / (P_c R_a)$$

This dimensionless group serves as the dimensionless group for the same initial condition. Thus, the following list constitutes the final similarity groups for the gravity drainage process being discussed:

$$\frac{\rho_1}{\rho_2}, \frac{\mu_2}{\mu_1}, \frac{\rho_1 g k}{\mu_1 u}, \frac{\rho_1 g L}{\sigma\sqrt{\frac{\phi}{k}}}, 2\sigma\cos\theta/(P_c R_a), \gamma(R_i)$$

1.7. Additional gravity drainage experiments

1.7.1 Scaled Physical Model of Gas-Assisted Gravity Drainage

The strategy for accomplishing the goal of constructing a scaled physical model study has been discussed in detail in the previous reports (152321R01, Rao et al., July, 2003). As mentioned in the previous progress report, the plan for the construction of the scaled physical model is in progress. Preliminary experiments are being conducted using a simple, unscaled physical model. The data obtained from the unscaled model and the theoretical analysis will be the platform for the development of the more realistic and representative *scaled* physical model. The existing model is a bead pack visual model. Glass beads of different sizes have been used for packing. The schematic of the existing model is shown in figure 1.10 below.

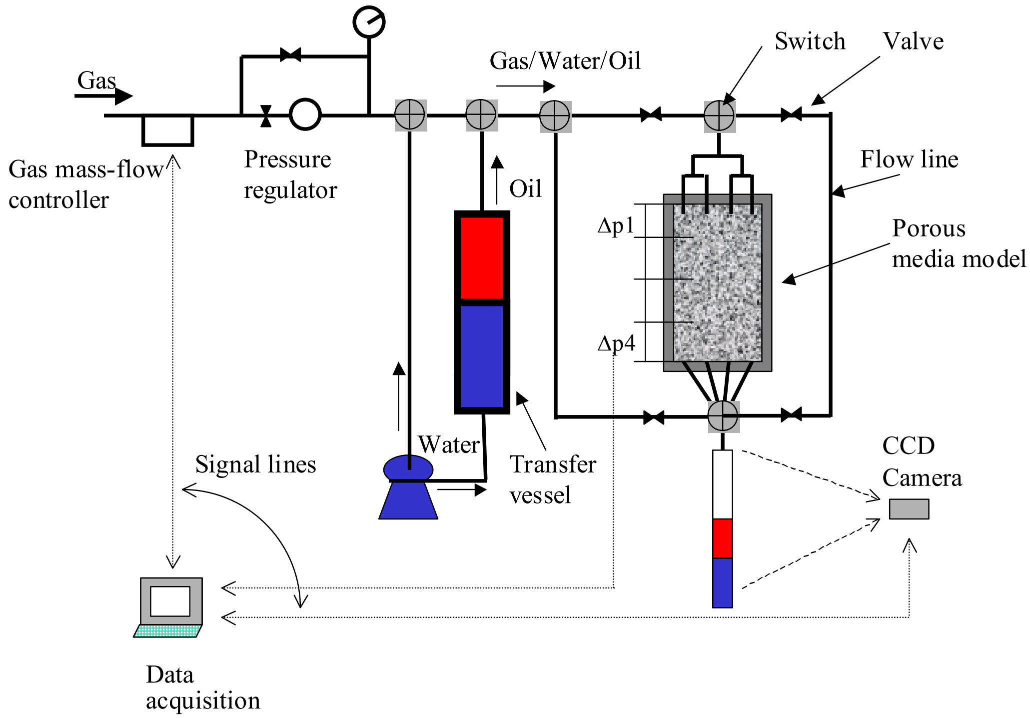

Figure 1.10 Schematic of the apparatus

As shown in the Figure 1.10, the apparatus consists of Pyrex glass windowed cell (packed with glass beads), transfer vessel, liquid pump, gas mass flow meter, a video recording system, pressure regulators and data acquisition systems. The cell is packed with glass beads and the assembly is tested for air tightness up to 10 psi. Mass flow controller provides the means of injecting gas at constant volumetric rate and measuring actual gas injection rate. A pressure regulator may be used at the gas supply outlet to conduct experiments with constant gas injection pressure. Effluent liquids are collected in a glass cylinder. A video system, which consists of a camera, frame grabber and imaging analysis software, is used to analyze oil and water production rates. The video system may also be used to analyze the interfaces of gas/water/oil inside the physical model. An automated computer-based measurement system is in the development stage for continuously monitoring the pressure, gas flow rate, and temperature.

In these tests, de-aerated water, paraffin (dyed red) and air have been used. Some physical properties of these three fluids are shown in Table 1.1.

Table 1.1. Fluids properties

Fluids	Specific density	Dynamic viscosity (cp) mPa•S	Interfacial tension (mN/m)
Paraffin	0.864	64.5	-
De-ionized Water	1	1.0	$\sigma_{WA} = 72$
Air	0.0012	0.0182	-

1.7.2 Experimental Strategies, Procedure, Results and Discussion

1.7.2.1 Experimental Strategies

The objectives of these experiments, as defined in the previous reports, are: investigating the gravity drainage behavior in a beadpack; identifying governing parameters (dimensionless groups) for the process; and gaining better understanding of the process to enable design and construction of a scaled physical model.

To investigate the response of the beadpack model, various parameters have been chosen as variables and experiments have been conducted to see how they affect the gravity drainage recovery process. The various variables identified till date are the gas infiltration rates, density, viscosity, interfacial tension, and grain size. Preliminary experiments have been conducted to study the recovery process using n-Decane (low viscosity of 0.84 cp), paraffin (high viscosity of 64.5 cp), coarse glass beads and fine glass beads.

The infiltrating gas velocities are classified as high, low and free gravity flow infiltrating velocities. Free infiltrating velocity refers to the case where the top of the model is opened for free infiltration of atmospheric air as liquid drains from the pack due to gravity. As reported earlier, free gas infiltration is actually a relatively rapid process due to the low viscosity of fluids and high permeability of the pack. The gravity drainage process may be applied to both waterflooded reservoirs and reservoirs with no prior waterfloods. To mimic these field situations, experiments have been conducted in different ways. For a gravity drainage scheme applicable to waterflooded reservoirs, the beadpack saturated with oil (n-decane/paraffin) is waterflooded in a gravity–stable mode from the bottom to the top of the model for a given duration of time, after which the water supply is cut-off. The top of the physical model is then opened for free gas invasion into the cell to assist gravity drainage of oil. This process will be referred to as *Tertiary Gravity Drainage*. Each run is conducted several times (at least two times) to see the reproducibility of the results. For a non-waterflood process, the oleic beadpack is opened to free air (Run#1) or subjected to constant pressure air injection (Run#5) and this process will be referred to as *Secondary Gravity Drainage*.

Table 1.2 shows the variables that are used for conducting the experimental runs during this quarter. The check marks indicate that the experiments have been completed. Paraffin was used as the oil in these sets of runs, and is referred to as high viscosity oil. Paraffin has a significantly higher viscosity as compared to n-decane (used in previous experiments), results from these experiments can be compared to see the effect of oil viscosity on recovery due to gravity drainage. All the experiments were carried out using coarse grain and paraffin as oleic phase. De-aerated water was used for saturating the model. Two of the four outlets provided in the physical model were kept open for all these runs for Gravity drainage of oil.

Table 1.2 Plan of Experiments with un-scaled physical model.

Run #	Size		Viscosity		Velocity			Waterflood		
	Large	Small	High	Low	High	Low	Free	Upward	Downward	Non
1	√		√				√			√
2	√		√				√			√
3	√		√				√	√		
4	√		√				√			√
5	√		√			√				√

1.7.2.2 Experimental Procedure

The beadpack physical model is saturated with brine, by imbibing brine from a burette placed at a sufficient level above the cell into the bottom of the cell. The transfer vessel is used for containing the hydrocarbons used (paraffin was used for these sets of experiments reported here). The liquid pump was used to transfer hydrocarbon from the transfer vessel to the top of the cell. Brine is drained from the bottom of the cell. The cell is saturated with hydrocarbon and connate water saturation is established. The cell is now ready for conducting gravity drainage experiments. As discussed earlier the various experiments conducted are all related to various production schemes associated with gravity drainage. Free gravity drainage, water flooding followed by free gravity drainage and gas assisted gravity drainage have been studied so far.

The experimental procedure for these experiments has been similar to that provided in the previous reports.

For convenience, paraffin is often referred as oil in the following text.

1. Imbibe de-ionized water into the pack from the bottom at a sufficiently large hydraulic head to ensure full saturation of water in the pack; record volume imbibed.

2. Displace water with oil downward at a constant injection rate until oil breaks through; record produced volume of oil.
3. Inject water at a constant rate into the pack downward or upward until water breaks through and oil production ceases off; record produced oil.
4. Open top and bottom of the model to atmosphere (Free gravity drainage) or connect the top of the model to air supply at constant pressure using a pressure regulator (Gravity drainage at low infiltration rate); collect effluent in a cylinder.
5. Monitor the volumetric increase of oil and water in cylinder using the Vision System.

For a non-waterflooded gravity drainage process, only step 3 is deleted from the above sequence.

The idea of the second step is to create an initial condition of oil saturated media with irreducible water saturation. Initial oil in place (IOIP), or paraffin in these experiments, is the total injected volume minus the produced oil volume,

IOIP = (pump flow rate × total time) – oil produced

1.7.2.3 Results and Discussion

Run# 1: Free Gravity Drainage: The aforementioned procedure was followed to carry out this run. A total of 555 cc of water was imbibed in the cell, attaining nearly 100% water saturation. Paraffin injection lasted for 60 minutes at a rate of 10 cc/min, during which a total of 600 cc of paraffin was injected. About 108 cc of paraffin was produced during injection. The total initial oil in place (IOIP) for this run was 490 cc. The S_o and S_{wi} were 88% and 12% respectively. The measuring cylinder was then calibrated with the vision system for recording the total volume of oil produced during gravity drainage. The detailed procedure for calibration of the vision system is discussed in the previous reports. Free gravity drainage was initiated by opening the two bottom ports and all the four top ports of the model for air infiltration. This run was not successful since poor images were received by the camera and the edge detector failed to record the proper oil production rates. Although, complete data was not obtained, the run was completed and the ultimate recovery was obtained. A total of 475 cc of oil was produced in less than 24 hours, generating a recovery of 96% IOIP. Figure 1.11 shows the total recovery vs. time for this run. The points on the X-axis appear because of the edge detector's failure to detect proper edges when a graduated glass cylinder was being used. This problem was solved later by using a measuring cylinder without marks, similar problem was observed till Run#3. This run was repeated to check for the repeatability and to obtain complete data.

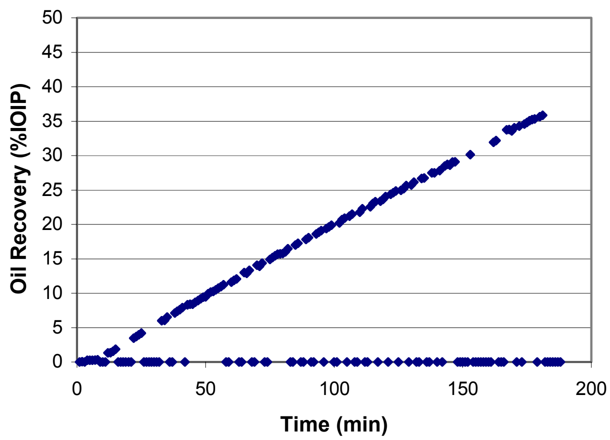

Figure 1.11. Experiment Run 1: Free gravity drainage

Run#2: (Repeat of Run 1) Free Gravity Drainage: This run was a repeat of Run#1. Similar procedure was used as in run#1 for conducting free gravity drainage of paraffin. 555 cc of water was imbibed in the cell, 500 cc of paraffin was used for drainage of water, 466 cc of paraffin was remaining in the cell, hence giving a total of 84% oil saturation and 16% irreducible water saturation. The vision system was calibrated and gravity drainage was initiated. The run was carried out for a total of 94 hours. An ultimate recovery of 89.05%IOIP was obtained. The total recovery of paraffin is plotted against the run in Figure 1.12. After point "A", immobile oil bank starts forming at the bottom of the cell, due to the capillary end effect, which arises from the oil film flow within the gas phase and results in an oil bank formation at the bottom of the cell. Once a high enough hydrostatic pressure is established in the cell that overcomes the capillary forces, the oil bank becomes mobile and starts flowing at a faster rate as indicated by point B of figure 1.12. The flow of oil starting from "B" lasts for a very short while, till the capillary end effect starts dominating the hydrostatic forces and results in lower flow rate out of the cell from "C" onwards. This phenomenon may re-occur again if the experiment were to be conducted for a longer periods of time.

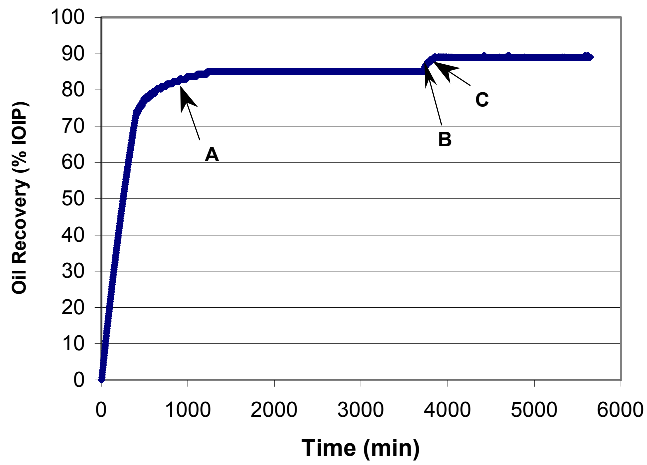

Figure 1.12. Experimental Run 2: Free gravity drainage

Run#3: Tertiary Gravity Drainage: This run was conducted to study the free gravity drainage in a waterflooded beadpack. The model was saturated with 528 cc of water. A total of 600 cc of oil was injected in the cell, leaving initial oil in place of 440 cc, and an irreducible water saturation of 16.6%. To mimic a secondary waterflood, the model was subjected to water injection from the bottom. 242 cc of oil was produced during water injection and 100 cc of water was produced after water breakthrough occurred in the model. Similar step jump as noticed in Figure 1.12 was noticed in this run as well, see figure 1.13. A total of 55% 0il recovery was obtained during the waterflood phase that lasted for 100 hours. After sufficient water has been produced during the waterflood phase, which indicates that the water oil ratio (WOR) is beyond the economic limits, the model was ready for free gravity drainage. Water supply was eliminated, and the top of the cell was subjected to free air intrusion. A total recovery of 30% of the IOIP was obtained for a run time of one hour, see figure 1.14. From the above results it can be inferred that gravity drainage on a waterflooded reservoir is comparatively faster than that in a non-waterflood reservoir. During the gravity drainage phase after waterflood, about 55% of the total waterflood recovery was obtained in less than 1/100th of the time required during the waterflood production. The ultimate recovery from this run was 85% of IOIP.

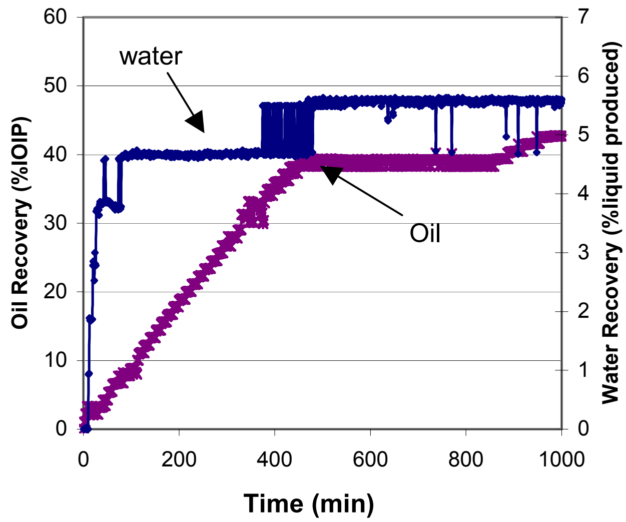

Figure 1.13. Run#3: Oil recovery during waterflooding

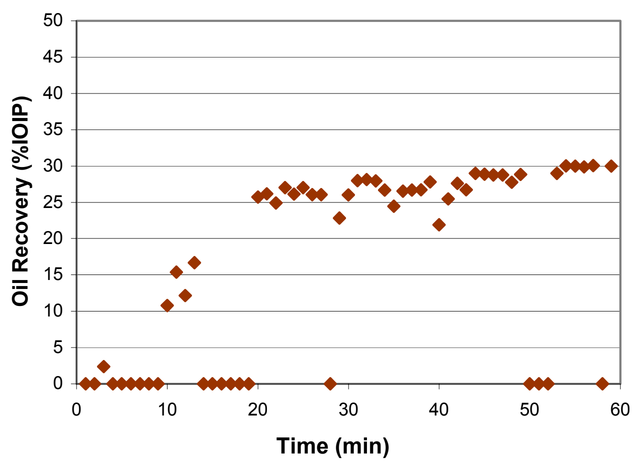

Figure 1.14. Run#3: Oil recovery during Tertiary Gravity Drainage

Run#4 Free Gravity Drainage: This run was carried out for the reproducibility of the results obtained in Run#2. Similar procedures were used. The model was imbibed with 534 cc of water. A total of 520 cc of oil was injected in the model and 30 cc of oil was produced during injection, leaving an IOIP of 490 cc and irreducible water saturation of 8.2 %. The ultimate recovery for this run was 78.9 % of IOIP as indicated in figure 1.15. Similar trend in oil recovery was obtained as was obtained in run#2. The ultimate recovery in this run this run was less than Run#2 because this run was carried terminated after 48 hours whereas Run#2 was carried out for 94 hours.

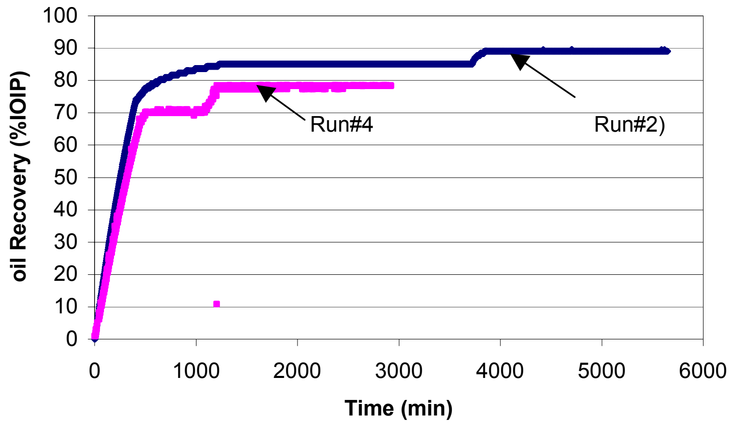

Figure 1.15. Run#4: Free Gravity Drainage (Repeat of Run 2)

Run#5: Secondary Gravity Drainage at Low Gas Infiltration Rates: The purpose of this run was to observe the recoveries when gas at constant pressure is injected in the model. In this run the same bead pack from previous run was used, initial oil (about 105 cc) from previous run was still present in the cell, most of which was concentrated at the bottom of the cell. A total of 392 cc of oil was injected and 37 cc of oil was produced during injection, leaving behind a total of 460 cc of IOIP. The top of the model was connected to air supply and a constant air injection pressure of 1 psig was used. The run was carried out for 64 hours. A plot of the recovery vs. time for this run is shown in Figure 1.16. Figure 1.16 indicates that the recovery from this run is slower as compared to that from free gravity drainage, which is contradictory to what should happen when gas at higher pressure is injected into the model. The possibility of error in this run maybe due to the pressure drop in the line from the air supply to the top of the cell. However the total recovery from this run was greater than that from the free gravity drainage.

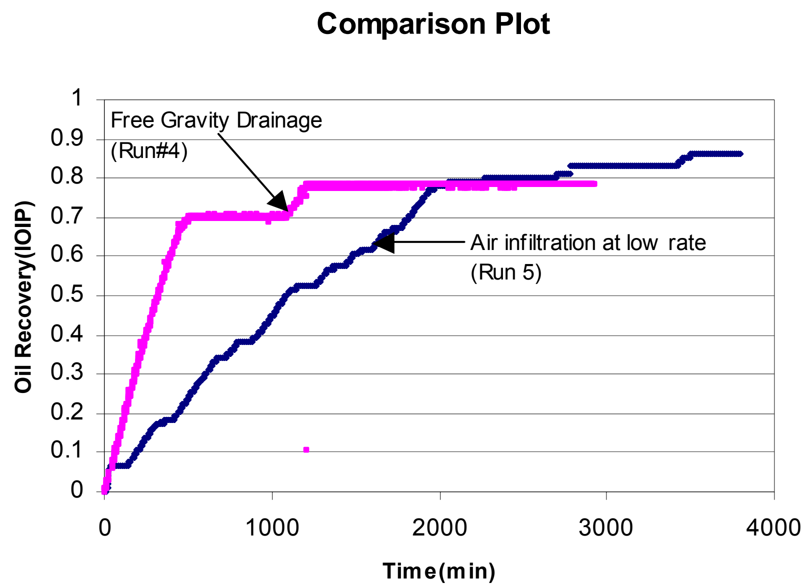

Figure 1.16. Run#5: Comparison of free gravity drainage and with gravity drainage at low infiltration rate

A summary of the results obtained in these experimental runs is provided below in Table 1.3. From table 1.3, it can be seen that the oil recovery from all these runs where not the same. Run#2 and 4 were repeated under similar conditions of free gravity drainage as Run#4. The Ultimate recovery from Run#2 was higher than Run#4, but the average production rate from Run#4 was higher than that from Run#2, this was because Run#4 had to be abandoned earlier. From Figure 1.15 it can be seen that similar production rates were obtained for the first ten hours when Run#4 was carried out (as a repeat of Run#2). The results from these experimental runs were found to be reproducible to some extent. Ultimate recovery for the Tertiary gravity Drainage process was similar to the free gravity drainage in Run#2. The initial production rates from Run#5 was observed to be comparatively smaller than Free gravity drainage, but the ultimate recovery as well as the production rates from this run was higher than Free gravity drainage.

Table 1.3: Summary of Results

Run #	Type of Run	IOIP (cc)	Initial oil saturation	Gravity drainage production (IOIP)	Ultimate recovery	
					IOIP	Time (Hours)
1	Free Gravity Drainage	460	88%	96	96	<24
2	Repeat of Run#1	466	84%	89	89	94
3	Tertiary Gravity Drainage	440	83.4%	85	85	100
4	Repeat of run#2	490	91.8%	78.9	72	48
5	Gravity Drainage at low infiltration rates	460	91%	86	86	63

Nomenclature

Consistent (e.g., SI) units are assumed in all equations in the text, SI units are listed below.

g = gravitational accelaration, m/s^2
k = permeability, m^2
k_r = relative permeability
K = spreading coefficient, dyne/cm
L = core length or length of section of core, m
p_i = pressure in phase i, Pa
$\Delta\mathscr{P}$= potential difference, Pa
R_i = Radii of a capillary tube, m
r = distance to center, m
S_w = water saturation
S_g = gas saturation
t = time, minutes
u_1 = oil superficial velocity, m/d
u_2 = gas superficial velocity, m/d
z = vertical coordinate ,cm

Greek Symbols

μ_1= oil viscosity, Pa s
μ_2= gas viscosity, Pa s
σ = interfacial tension, dyne/cm
$\gamma(R_i)$ = pore throat size distribution function
ρ = density, kg/m^3
θ = contact angle
ϕ = porosity

References:

Bakke, S. and Øren, P. E., "3-D Pore-Scale Modeling of Sandstones and Flow Simulations in the Pore Neqworks," *SPE J* (1997) No. **2**, p. 136-149.

Bryant, S. and Blunt, M., "Prediction of Relative Permeability in Simple Porous-Media," *Physical Review A* (1992) **46**, No. 4, p. 2004-2011.

Buckley, S. E. and Leverett, M. C., "Mechanism of fluid displacement in sands," *Trans., AIME* **146**, 107 (1941)

Cardwell, N. T., and Parsons, R. L., "Gravity Drainage Theory," *Trans. AIME* (1949), **179**, 199-215.

Da Sle, W. J., and Guo, D. S., "Assessment of a Vertical Hydrocarbon Miscible Flood in the Westpem Nisku D Reef," *SPERE* (May 1990) 147-154.

DesBrisay, C. L., Ghussein, F. E., and Holst, P. H., "Review of Miscible Flood Performance, Intisar "D" field, Socialist People's Libyan Arab Jamahiriya," SPE 10245, presented at the 56th Annual Fall Technical Conference and Exhibition of the Society of Petroleum Engineers of AIME, held in San Antonio, Texas, October 5-7, 1981.

DiCarlo, D. A., Sahni, A., and Blunt, M., "Three-Phase Relative Permeability of Water-wet, Oil-wet, and Mixed-Wet Sandpacks," *SPE J.*, March 2000.

Grattoni, C. A., Jing, X. D., and Dawe, R. A., "Dimensionless Groups for Three-Phase Gravity Drainage Flow in Porous Media," *J. Pet. Sci. & Eng*. **29** (2001) 53-65.

Hagoort, J., "Oil Recovery by Gravity Drainage," *SPE J.* (June 1980) 139-150.

Kantzas, A., Chatzis, I., and Dullien, F. A. L., "Mechanisms of Capillary Displacement of Residual Oil by Gravity-Assisted Inert Gas Injection," SPE 17506, This paper was prepared for presentation at the SPE Rocky Mountain Regional Meeting, held in Casper, WY, May 11-13, 1988.

Lake, L. W., "Enhanced oil recovery," Prentice Hall, Englewood Cliffs, NJ (1989).

Luan, Z., "Some Theoretical Aspects of Gravity Drainage in Naturally Fractured Reservoirs," SPE 28641, this paper was prepared for presentation at the SPE 69th Annual Technical Conference and Exhibition held in New Orleans, LA, U.S.A., 25-28 September 1994.

Rao, D., Xu, Q., Ayirala, S., and Kulkarni, M., "Development and Optimization of Gas-Assisted Gravity Drainage Process for Improved Light Oil Recovery," Quarterly Technical Progress Report to the U. S. Department of Energy, 2003.

Nutt, C. W., "The Physical Basis of the Displacement of Oil from Porous Media by other Fluids: a Capillary Bundle Model," *Proc. Roy. Soc. Lond.*, **A382**, 155-178, 1982.

Ypma, J. G. J., "Analytical and Numerical Modeling of Immiscible Gravity-Stable Gas Injection into Stratified Reservoirs," *SPE J*. (Aug. 1985) 554-564.

II. Further Development of the Vanishing Interfacial Tension (VIT) Technique

In the last progress report (Report #15323R02, July 2003), under this section, the effect of tuning Equation of State (EOS) on minimum miscibility pressure (MMP) calculations was presented and the results were reported for two real reservoir cases, namely Rainbow Keg River (RKR) and Terra Nova. These results implied that tuning of EOS is not suitable for miscibility calculations of these two reservoirs. Also, interfacial tension (IFT) measurements were reported for a standard liquid ternary system of ethanol, water and benzene at ambient conditions. The comparison of these IFT measurements with the solubility data demonstrated not only different regions of solubility characteristics but also the applicability of the new VIT technique even for ternary liquid systems. In addition, the progress in the design and assembly of experimental system to be used for IFT measurements at actual reservoir conditions was reported. The research work done further under Task 2 during the last quarter is divided mainly into the following four sections:

1. Comparison of VIT experimental interfacial tension measurements with Weinaug and Katz's parachor computational model for RKR reservoir fluids
2. Effect of gas/oil ratio (GOR) on IFTs determined from parachor computational model for RKR reservoir fluids
3. Comparison of VIT experimental MMPs with EOS calculations and parachor computational model for RKR fluids to estimate the extent of mass transfer involved in each of these MMP determination methods
4. Progress in the IFT measurements of standard ternary liquid system at ambient conditions

2.1 Comparison of Gas/Oil IFT Measurements with Parachor Model

2.1.1 Introduction

Interfacial tensions are highly important for processes such as gas injection and flow through porous media. Therefore, simple and accurate computational models for IFT prediction are required. In the last few decades, several models have been proposed for IFT calculations. The most important among these models are the parachor method (Macleod, 1923, Sudgen 1924), the corresponding states theory (Brock and Bird, 1955), thermodynamic correlations (Clever and Chase 1963) and the gradient theory (Carey, 1979). The present study of IFT calculations is initiated with the parachor method.

<u>Parachor Method</u>:

The Macleod-Sudgen (Macleod, 1923, Sudgen, 1924) correlation relating the vapor liquid interfacial tension of a pure compound to the density difference is given as

$$\sigma^{1/4} = P_\sigma (\rho_M^L - \rho_M^V) \qquad (2.1)$$

where ρ_M^L and ρ_M^V are the molar density of the liquid and vapor phase, respectively in gmole/cm^3 and σ is the interfacial tension in mN/m.

The proportionality constant, P_σ is called the parachor, a parameter representing the molecular volume of a compound under the conditions where the effect of temperature is neutralized. It is considered to have a unique value for each hydrocarbon compound independent of pressure and temperature. The parachor values of different pure compounds are determined from the interfacial tension measurements, using the Macleod-Sudgen equation. The values of parachors were reported in the literature by several investigators (Quale, 1953, Fanchi, 1990, Ali, 1994, Schechter and Guo, 1998).

The Macleod-Sudgen equation was extended to hydrocarbon mixtures using Weinaug and Katz's (Weinaug and Katz, 1943), simple molar averaging technique for the mixture parachor,

$$\sigma^{1/4} = \rho_M^L \sum x_i P_{\sigma i} - \rho_M^V \sum y_i P_{\sigma i} \qquad (2.2)$$

where, x_i and y_i are the mole fractions of component i in the liquid and vapor phases respectively and $P_{\sigma i}$ is the parachor of the component i .

2.1.2 Objective

The objective is to compare the VIT experimental interfacial tension measurements with Weinaug and Katz's parachor model. For this purpose, RKR reservoir was used, since the temperature, crude oil and solvent compositions needed for IFT calculations and the VIT experimental IFT values were available for this reservoir (Rao, 1997, Rao et al., 1999).

2.1.3 Methodology

10 mole% crude oil and 90 mole% solvent was used as the feed composition in the IFT computational model as similar feed conditions were used in VIT experiments. Flash calculations were performed with the mixed feed at the specified pressure and reservoir temperature at varying C_{2+} enrichments in solvent. The resultant molar liquid, vapor densities, equilibrium liquid and vapor compositions of different components along with their parachors reported in literature, were used in IFT computations. All these calculations were based on untuned PR- EOS, within a commercial simulator.

2.1.4 Results and Discussion

The comparison of VIT experimental IFTs with Weinaug and Katz's parachor computational model for RKR fluids at different C_{2+} enrichments in solvent is shown in Figures 2.1 and 2.2, respectively at pressures 14.8 MPa and 14.0 MPa. As can be seen in these figures, similar trends were observed at both the pressures. The parachor computational model under predicts the interfacial tension in high IFT regions. However, the difference between the experimental and the calculated IFTs gradually decreases and consequently the parachor model predictions match the VIT experiments in low IFT regions. This is in good agreement with Cornelisse et al. (1993), who made similar observations. This implies that the parachor computational model can be used for predicting the low IFTs of these reservoir fluids.

2.2 Effect of GOR on IFTs Determined from Parachor Model

Different feed conditions of (1 mole% oil + 99 mole% solvent), (10 mole% oil + 90 mole% solvent), (20 mole% oil + 80 mole% solvent), (40 mole% oil + 60 mole% solvent), (60 mole% oil + 40 mol% solvent), (80 mol% oil + 20 mole% solvent) and (90 mole% oil + 10 mole% solvent) were used to study the effect of gas/oil ratio on IFTs determined from parachor computational model for RKR reservoir. The methodology described in Section 2.1.3 of this report holds good even for this case.

2.2.1 Results and Discussion

The calculated IFTs as a function of C_{2+} enrichment in solvent, at different feed conditions for RKR fluids is shown in Figures 2.3 and 2.4, respectively for pressures 14.8 MPa and 14.0 MPa. As can be seen in these figures, the trends were similar for both the cases. The calculated IFTs decrease with the increase of GOR at a given C_{2+} enrichment in solvent. The IFTs followed a gradual smooth trend to the point of zero interfacial tension only for the feed conditions of (10 mole% oil + 90 mole% solvent) and (20 mole% oil + 80 mole% solvent). For all the remaining feed conditions except at the feed conditions of (80 mole% oil + 20 mole% solvent) and (90 mole% oil + 10 mole% solvent), the IFTs gradually declined up to a certain value and then suddenly dropped to the point of zero IFT. For the feed conditions of (80 mole% oil + 20 mole% solvent) and (90 mole% oil + 10 mole% solvent), the calculated IFTs are almost insensitive to C_{2+} enrichment in solvent and hence never reached the point of zero interfacial tension. These observations appear to indicate some kind of computational instability in the calculation procedure of parachor models.

2.3 Comparison of VIT MMPs with EOS Calculations and Parachor Models

2.3.1 MMP Determination using EOS

The following steps are used in the commercial simulator to calculate the MMPs using untuned PR-EOS at the reservoir temperature.

1. Choose an initial pressure below MMP.
2. Input temperature, crude oil composition, primary and makeup gas compositions, makeup gas fraction, pressure increment, solvent to oil ratio increment, equilibrium gas/original oil mixing ratio and equilibrium liquid/original solvent mixing ratio.
3. Mixing primary gas with a specified mole fraction of make-up gas forms the solvent.
4. Solvent is added to oil at specified solvent to oil molar ratio increments and flash calculations are performed until two-phase region is detected. The absence of two-phase region implies first contact miscibility and the program stops.
5. For the two- phase region presence, the program checks the relative positions of injected gas composition and crude oil composition with respect to limiting tie line. If the injected gas composition is to the left, while that of crude oil to the right of limiting tie line, then the process is vaporizing gas drive or else, the process is condensing gas drive.
6. For vaporizing gas drive, using the first point in the two-phase region detected in step 4, the flashed vapor is mixed with the original oil at the specified equilibrium gas/original oil mixing ratio and the flash calculation is performed.
7. For condensing gas drive, using the first point in the two-phase region detected in step 4, the flashed liquid is mixed with the original solvent at the specified equilibrium liquid/original solvent mixing ratio and the flash calculation is performed.

8. The procedure is repeated until the liquid composition is same as the vapor composition and MMP is the pressure at which this occurs and the program stops.
9. If it is not true, then the pressure is increased at the specified pressure increment and the steps 4 to 8 are repeated.

2.3.2 MMP calculation using Parachor Computational Model

The sequence of steps followed in MMP calculation procedure using parachor computational model are:

1. Input oil composition, solvent composition, reservoir temperature, mole fraction of oil in the feed, pressure and the pressure increment.
2. Perform flash calculations using untuned PR-EOS with mixed feed at reservoir temperature and specified pressure.
3. The resulting molar liquid, vapor densities, equilibrium liquid and vapor compositions of different components along with their parachors were used to calculate the IFTs.
4. The pressure is incremented at the specified pressure increment and the steps 2 to 3 are repeated.
5. The calculated IFTs are then plotted against pressure and the extrapolation of the data to zero interfacial tension gives the MMP.

2.3.3 Results and Discussion

The summary of VIT experimental MMPs, EOS calculated MMPs and the MMPs from parachor computational model for RKR fluids at C_{2+} enrichments of 51.0% and 52.5% in solvent is given in Table 2.1. The calculated IFTs using the parachor computational model at these C_{2+} enrichments are plotted against pressure to determine MMPs in Figure 2.5. As can be seen in Table 2.1, similar trends were observed at both the C_{2+} enrichments. The VIT experimental MMPs are lower than EOS calculated MMPs, which in turn are lower than the MMPs from parachor computational model. The possible explanation for this is given below.

Since VIT data is based on actual experiments, all directions of mass transfer are allowed to take place (condensing gas drive, vaporizing gas drive and combined condensing/vaporizing gas drive). However, in EOS calculations, only limited mass transfer is taken into account through either condensing gas drive or vaporizing gas drive in the calculation procedure, which over predicts the MMP. Furthermore, in parachor computational model, any type of mass transfer is not considered at all due to the absence of these drive mechanisms in the calculation procedure, which over predicts the MMP even further. Therefore, it appears that the ability of any miscibility computational procedure to account for the mass transfer effects between the fluids governs the extent of agreement with miscibility determined from VIT experiments.

2.4 IFT Measurements of a Standard Ternary Liquid System

The ambient IFT experiments conducted so far for the standard ternary liquid system of ethanol, water and benzene indicated the applicability of the new VIT technique to determine the miscibility of ternary liquid systems. However, this is not completely validated due to the inability to measure the low IFTs at ethanol enrichments of above 40 mole% with the available Axisymmetric Drop Shape Analysis (ADSA) technique. This necessitated the need to identify another experimental technique for measuring low IFTs at ethanol enrichments of above 40 mole% to clearly determine the point of vanishing IFT enrichment for benzene-water-ethanol system. In the present study, capillary rise technique is identified as the potential means to measure the very low IFTs needed to validate the VIT technique for ternary liquid systems.

2.4.1 Capillary Rise Technique

The force balance in a capillary is given by,

$$2\pi r\sigma\cos\theta = \pi r^2 h\Delta\rho\frac{g}{g_c} \quad \text{……} \quad (2.3)$$

Solving for interfacial tension, σ, gives

$$\sigma = \frac{rh\Delta\rho g}{2\cos\theta g_c} \quad \text{……} \quad (2.4)$$

where, σ = interfacial tension in $dynes/cm$

r = pore throat radius in cm

h = capillary rise in cm

Δρ = density difference between the fluids in gms/cc

θ = equilibrium contact angle in degrees

g = acceleration due to gravity (980 $cm/\sec^2$)

g_c = conversion (1 $\frac{gm.cm/\sec^2}{dyne}$)

The parameters to be measured experimentally to compute the interfacial tension by this technique are the capillary rise, h and the equilibrium contact angle, θ.

The capillary rise to be measured using the image analysis software, which detects the interface due to the contrast in color. Then, the rise can be measured in real units by calibrating the reference object of known length in the image. The detailed description of this analysis is provided in Section 1.2.3 of the progress report (Report #15323R02, July 2003).

The equilibrium contact angles are to be measured using the existing dual drop dual crystal ambient cell, fluids of interest and the substrate with which the capillary tubes are made.

2.5 Conclusions

2.5.1 Comparison of Gas/Oil IFT Measurements with Parachor Model

1. Parachor computational models under predict IFT in high IFT regions.
2. In low IFT regions, parachor computational model predictions match with VIT experiments.
3. Parachor computational models can be used to predict the low IFTs of RKR fluids.

2.5.2 Effect of GOR on IFTs Determined from Parachor Computational Model

1. The calculated IFTs decrease with the increase of GOR at a given C_{2+} enrichment in solvent.
2. The IFTs followed a smooth gradual trend to the point of zero interfacial tension at gas oil ratios of only (10 mole% oil + 90 mole% solvent) and (20 mole% oil + 80 mole% solvent) in the feed.
3. At all the other gas oil ratios, the IFTs either suddenly drop to the point of zero IFT or insensitive to C_{2+} enrichment in solvent and never reach the point of zero IFT.
4. These observations clearly appear to indicate some kind of computational instability in the calculation procedure of parachor models.

2.5.3 Comparison of VIT MMPs with EOS Calculations and Parachor Models

1. EOS calculations and parachor computational models over predict MMPs.
2. The over predictions appear to be due to the inability of these calculation procedures/computational models to account for all the mass transfer effects that can occur in reality between the fluids.
3. This gives raise the need to develop methods to incorporate all the mass transfer effects in the calculation models to determine fluid-fluid miscibility. The analytical technique of tie-line length calculation (Wang and Orr, 1998) appears to offer one such route.

2.5.4 IFT Measurements of a Standard Ternary Liquid System

1. Capillary rise technique is identified as the potential mode to measure the very low IFTs needed to validate the VIT technique for ternary liquid systems.
2. The capillary rise will be measured using the image analysis.
3. The equilibrium contact angles are being measured using the dual drop dual crystal ambient cell.

2.6 Future Plans

1. Literature review on IFT computational models.
2. To experimentally measure the low IFTs above 40 mole% ethanol enrichment using capillary rise technique for benzene-water-ethanol system to clearly validate the applicability of VIT technique to determine the miscibility of ternary liquid systems.
3. To experimentally investigate the effect of solvent/oil ratio on IFT measurements of benzene-water-ethanol system.

Table 2.1: Comparison of VIT MMPs with EOS Calculations and Parachor Models for RKR Fluids

MMP Determination Method	Solvent #1 (C_{2+} = 51.0 %) MMP (MPa)	Solvent # 2 (C2+ = 52.5%) MMP (MPa)
Experimental (VIT)	14.8	14.0
EOS calculation	17.8	16.7
Parachor computational model	19.3	18.6

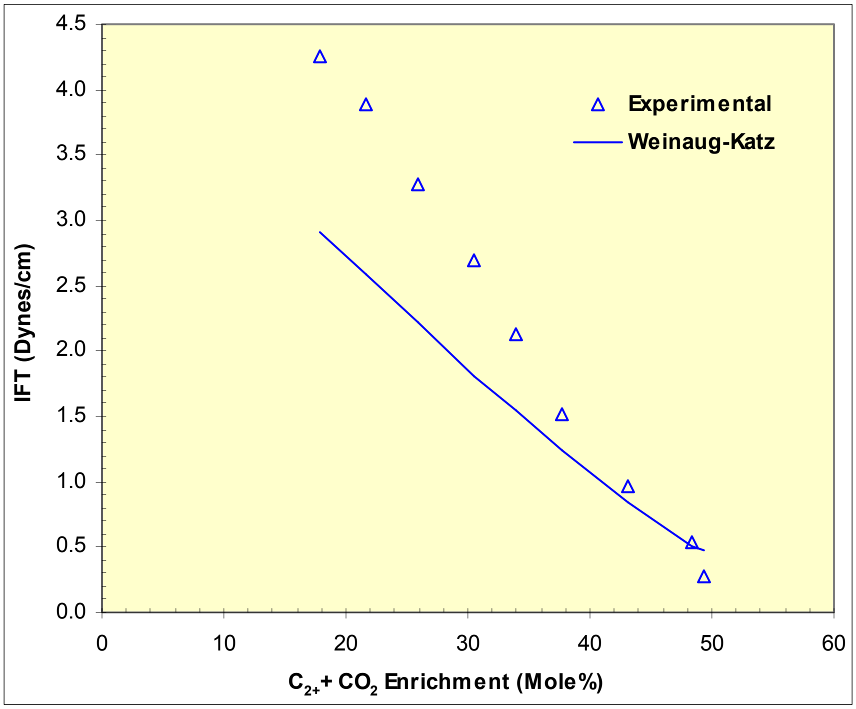

Figure 2.1: Comparison of VIT Experimental IFTs with Parachor Computational Model for RKR Fluids at a Pressure of 14.8 Mpa

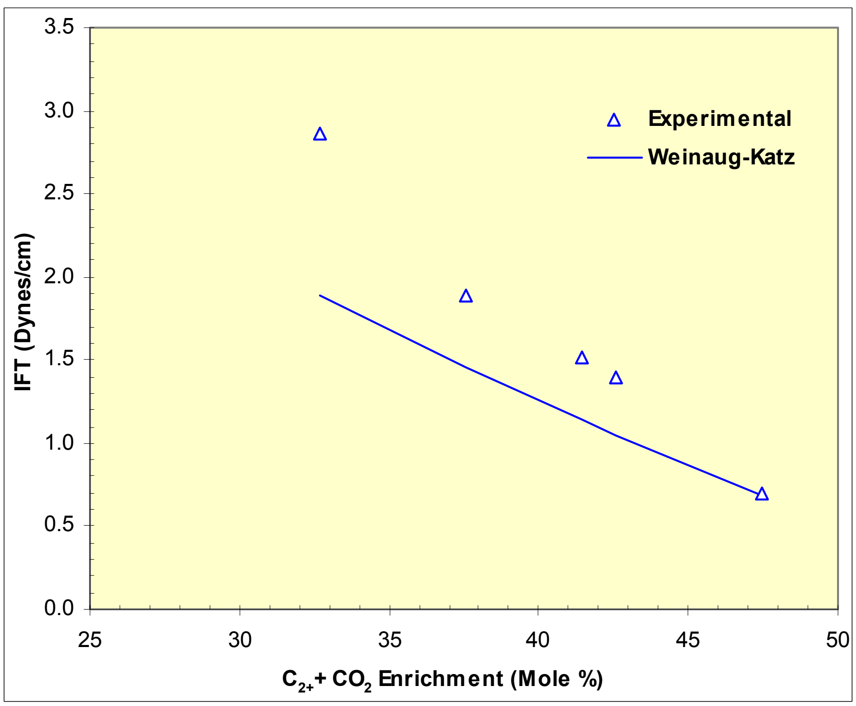

Figure 2.2: Comparison of VIT Experimental IFTs with Parachor Computational Model for RKR Fluids at a Pressure of 14.0 MPa

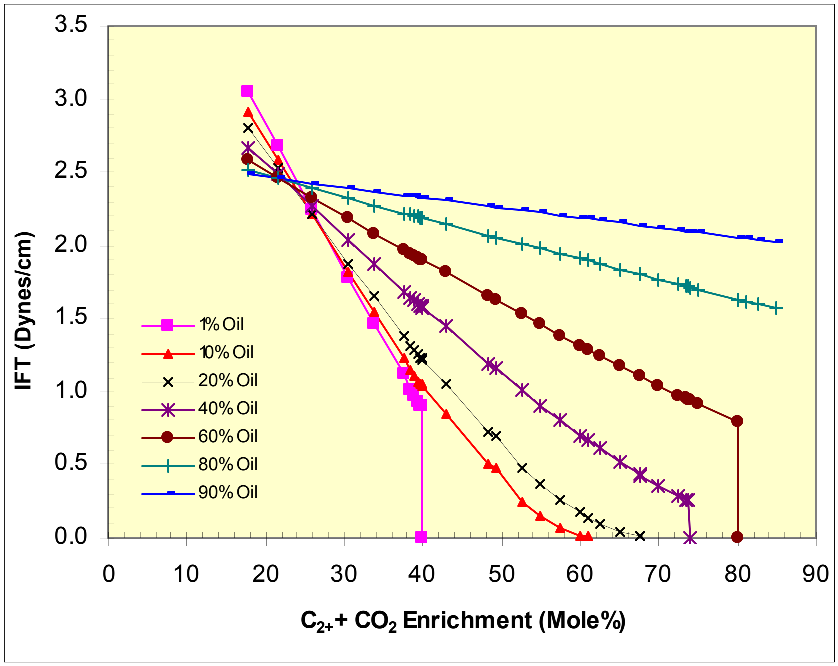

Figure 2.3: Effect of GOR on Parachor Computational Model IFTs for RKR Fluids at a Pressure of 14.8 MPa

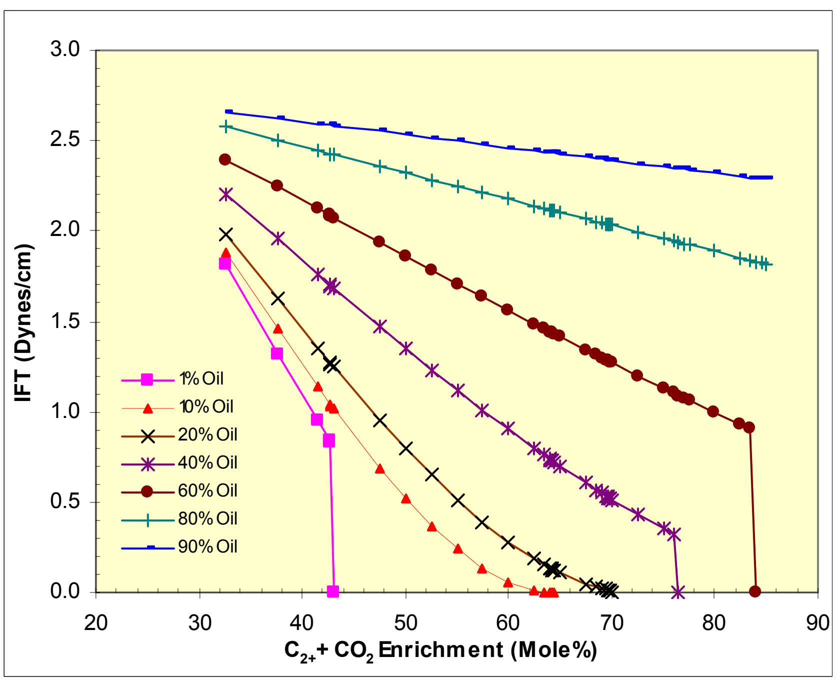

Figure 2.4: Effect of GOR on Parachor Computational Model IFTs for RKR Fluids at a Pressure of 14.0 MPa

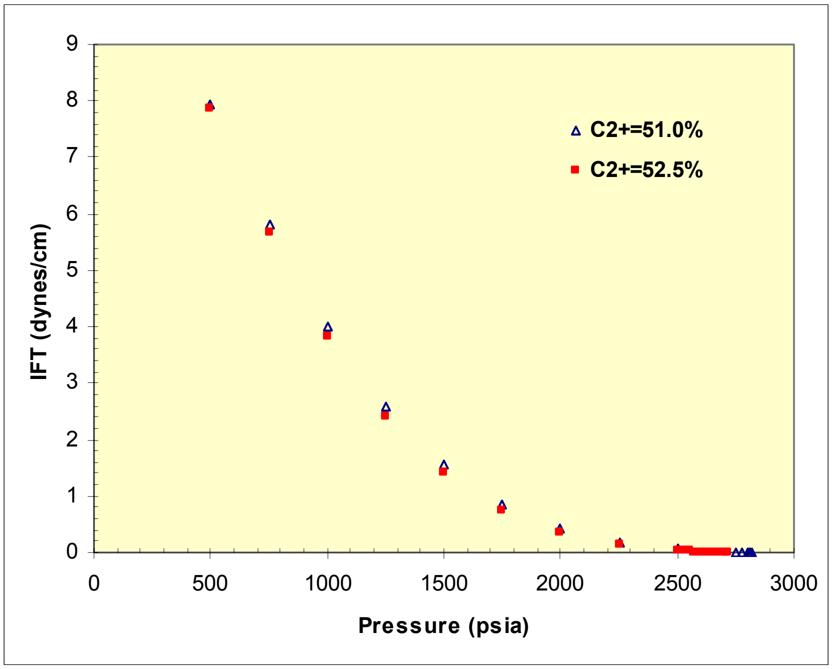

Figure 2.5: MMP Determination Using Parachor Computational Model for RKR Fluids

References:

Ali, J.K.: "Predictions of Parachors and Petroleum Cuts and Pseudo Components," *Fluid Phase Equilibria,* **95** (1994) 383-398.

Brock, H.L. and Bird, R.B.: "Surface Tension and Principle of Corresponding States," *AIChE J*., **1** (1955) 174-177.

Carey, B.S.: "The Gradient Theory of Fluid Interfaces," *PhD Dissertation* (1979), University of Minnesota, Minneapolis.

Clever, H.L. and Chase, W.E., Jr.: "Thermodynamics of Liquid Surfaces, Surface Tension of n-hexane-cyclohexane mixtures at 25, 30 and 35^o C," *J. Chem. Eng. Data*, **8** (1963) 291-292.

Cornelisse, P.M.W., Peters, C.J. and de Swaan Arons, J.: "Application of the Peng-Robinson Equation of State to Calculate Interfacial Tensions and Profiles at Vapor-Liquid Interfaces," *Fluid Phase Equilibria*, **82** (1993) 119-129.

Fanchi, J.R.: "Calculation of Parachors for Compositional Simulation: An Update," *SPE Reservoir Engineering*, (1990) 433-436.

Macleod, D.B.: "On a Relation Between Surface Tension and Density," *Trans. Faraday Soc*., **19** (1923) 38-42.

Quale, O.R.: "The Parachors of Organic Compounds," *Chem. Review,* **53** (1953) 439-586.

Rao, D.N.: "A New Technique of Vanishing interfacial Tension for Miscibility Determination," *Fluid Phase Equilibria*, **139** (1997) 311-324.

Rao, D.N., Mcintyre, F.J., and Fong D.K.: "Application of a New Technique to Optimize Injection Gas Composition for the Rainbow Keg River F Pool Miscible Flood," *JCPT,* **38** (1999) 1-10.

Rao, D.N., Xu, Q., Ayirala, S.C. and Kulkarni, M.M.: "Development and Optimization of Gas Assisted Gravity Drainage (GAGD) Process for Improved Light Oil Recovery," Quarterly Technical Progress Report, Report # 15323R02, July 2003.

Schechter, D.S. and Guo, B.: "Parachors Based on Modern Physics and Their Uses in IFT Prediction of Reservoir Fluids," *SPE Reservoir Evaluation & Engineering*, (1998) 207-217.

Sudgen, S.: "The Variation of Surface Tension with Temperature and Some Related Functions," *Journal of Chemical Society*, (1924) 32-41.

Wang, Y. and Orr, F.M., Jr.: "Calculation of Minimum Miscibility Pressure," Paper SPE 39683 Presented at the 1998 SPE/DOE Improved Oil Recovery Symposium, Tulsa, OK, April 19-22.

Weinaug, C.F. and Katz, D.L.: "Surface Tensions of Methane-Propane Mixtures," *Industrial Engineering Chemistry*, **35** (1943) 239-246.

III. Determination of Multiphase Displacement Characteristics In Reservoir Rocks

The study of WAG process and the results of multi-phase displacement experiments conducted along with the detailed literature review, experimental apparatus and experimental design aspects of Task 3 were included in the previous progress reports to DOE, 15323R01, (April 2003) and 15323R02 (July 2003). The present report not only augments the previous work of evaluation of the multiphase displacement characteristics of reservoir (Berea) rocks, but also extends it to 'Hybrid' WAG and gravity stable type multi-phase displacements in the laboratory using Berea sandstone cores. This report also reports on the investigation of the recommendations and hypotheses resulting from the previous work.

This report covers the work completed in the fourth quarter of the project (Jul-Sept 2003) and includes: Introduction to gravity stable gas injection processes, extensive literature review, experimental work update, future plans and updated experimental protocol.

3.1 Abstract

Gas injection has proved its potential as a powerful EOR process. Numerous field applications to almost all reservoir types and reservoirs with varying residual oil saturations stand testimony to this statement. The gas injection processes have high microscopic sweep efficiencies but demonstrate poor volumetric sweeps (due to severe gravity segregation) in horizontal floods due to the unfavorable mobility ratio between the injected gas and reservoir fluids. Water-Alternating-Gas method, the most popular sweep improvement method in the oil field, to date, however, has shown disappointing results like poor reservoir sweep efficiencies and lower recoveries (5-10% OOIP) (Rao, 2001). Other volumetric sweep improvement methods like the Denver Unit WAG (DUWAG), Simultaneous WAG (SWAG), gas (CO_2) thickeners, foam injection etc. have had limited success (Moritis, 1995).

All these methods are still aimed at overcoming the gravity force (consequently the natural phenomenon of gravity segregation) and an 'attempt' to improve the flood profile (Moritis, 1995). Additionally, WAG results in increased mobile water saturation in the reservoir leading to increased water shielding and decreased gas injectivity in the reservoir.

Up dip gas injection into dipping reservoirs is one of the most efficient methods to recover waterflood residual oil. Corefloods and field investigations confirm that a large amount of incremental tertiary oil can be recovered using gravity assisted tertiary gas injection. Recoveries as high as 85 – 95% OOIP have been reported in field tests and nearly 100% recovery efficiencies have been observed in laboratory floods.

This study is directed toward the evaluation of the Gas Assisted Gravity Drainage (GAGD) process, its design parameters and the associated rock-fluid interactions in the laboratory. Literature review suggests that the important reservoir/rock-fluid design parameters for a successful gravity assisted gas injection process include: reservoir fluids spreading coefficient, reservoir heterogeneity, operational pressure, slug composition and size, stable frontal advancement rate (injection rate), oil relative permeability, three-phase relative permeability effect, reservoir capillary pressure, oil film flow rates, reservoir dip, and waterflood residual oil saturation.

Previous WAG studies (reported in our earlier reports) have suggested the use of 'Hybrid'-WAG type floods for improved CO_2 utilization factors and recoveries. These as well as the effect of saturating the injection water with CO_2 for corefloods have been investigated further in this quarter. Evaluation of the multiphase displacement characteristics by conducting corefloods, both 'Hybrid'-WAG and gravity stable type, in Berea sandstone cores using synthetic as well as real reservoir fluids are planned for the next quarter. Miscible and immiscible floods with Berea sandstone cores using n-Decane, Yates reservoir brine and Yates crude oil with pure CO_2 injectant are also planned as future tests.

3.2 Research Focus

The research focus for this reporting quarter was the further investigation of the recommendations of the previous experimental investigations and are summarized below:

1. Literature update to include gravity drainage laboratory/theoretical and field studies to identify the design parameters affecting gravity drainage.
2. Investigation of the delayed breakthrough observed in the previous coreflood studies by studying the system behavior with CO_2-saturated Yates brine.
3. Further investigation of the predicted optimum 'Hybrid WAG' type injection by conducting 'Hybrid WAG' type corefloods using both CO_2-saturated as well as unsaturated brine.
4. To conduct high-pressure corefloods (CGI/WAG/Hybrid-WAG/GAGD modes of gas injection) in both immiscible and miscible modes with Berea cores at reservoir conditions.

3.3 Literature Review

Extensive literature review to study the displacement characteristics (instabilities and critical rates), laboratory studies and field applications for gravity drainage has been completed. The comprehensive literature review is included as Appendix 1 to this report, and a brief summary is provided below.

3.3.1 Summary of Laboratory and Theoretical Studies

Displacement instabilities in gravity drainage are a function of rock-fluid properties, fluid saturation distributions, the viscous forces and rock-fluid and fluid-fluid interaction parameters such as rock wettability, interfacial tension and miscibility. Fluid cross flow and mixing of the miscible slug and chase gas results in displacement instabilities consequently reducing the displacement efficiency. Also the 3-phase relative permeability effects (especially oil relative permeability) and film flow are critical for stable displacements and higher recoveries.

Another important parameter determining the stability of the growing interface and preventing coning or cresting is the critical gas injection rate. Injection rates above the critical results in 'short-circuiting' of the injected gas to the production well drastically reducing sweep. Modeling studies have shown that shorter well spacing aids the displacement front stability. Both the displacement instabilities and critical injection rates are important for flood profile control and need to be evaluated using 3D physical models and in reservoir simulation.

Miscibility between the injected gas and reservoir fluid helps the reduction of viscous displacement instabilities by reducing the fingering. Furthermore miscibility development lengths are shorter in gravity-assisted floods than horizontal floods helping better gas-oil contacts in the reservoir.

Significantly high recoveries in gravity drainage reservoirs are possible in strongly water-wet systems with positive oil spreading coefficient. Micromodel studies show that positive spreading coefficients are obtainable under strongly water-wet conditions, where continuous oil films over water is obtainable in gas swept zones.

Vertical coreflood displacement studies suggest the preference to the use of CO_2 over hydrocarbon gases due to the higher recovery efficiency and injectivity characteristics of CO_2; although economical and assured supply of CO_2 for EOR applications could be an issue.

3.3.2 Summary of Field Applications

Table 1 shows the summary of the field applications studied for the literature review. Table 2 shows the 'vertical' gravity stable hydrocarbon (HC) miscible floods conducted during 1964 – 1987 in Canada. The important inferences from field applications are summarized below.

Table 1: Summary of Gravity Drainage Field Applications Studied

Property	West Hackberry	Hawkins Dexter Sand	Weeks Island S RB - Pilot	Bay St. Elaine	Wizard Lake D3A	Westpem Nisku D	Wolfcamp Reef	Intisar D	Handil Main Zone
State / Country	LA	Texas	LA	LA	Alta	Alta	TX	Libya	Borneo
Rock Type	Sand-Stone	Sand-stone	Sand-stone	Shly-Sand	Dol-omite	Carb-onate	Lime-Stone	Biomicrite/Dolo.	Sand-stone
Porosity (%)	27.6 – 23.9	27	26	32.9	10.94	12	8.5	22	25
Permeability (mD)	300 – 1000	3400	1200	1480	1375	1050	110	200	10 – 2000
Connate Water Sat. (%)	19 – 23	13	10	15	5.64	11	20	N/A	22
WF Residual Oil Sat. (%)	26	35	22	20	35	N/A	35	N/A	N/A
GI Residual Oil Sat. (%)	8	12	1.9	N/A	24.5	5	10	N/A	N/A
Reservoir Temperature (°F)	205 – 195	168	225	164	167	218	151	226	N/A
Bed Dip Angle (Degrees)	23 – 35	8	26	36	Reef	Reef	Reef	Reef	5 – 12
Pay Thickness (ft)	31 – 30	230	186	35	648	292	824	950	15 – 25 (m)
Oil API Gravity	33	25	32.7	36	38	45	43.5	40	31 – 34
Oil Viscosity (cP)	0.9	3.7	0.45	0.667	N/A	0.19	0.43	0.46	0.6 – 1.0
Bubble Pt Pressure (psi)	3295	1985	6013	N/A	2154	3966	1375	2224	2800– 3200
GOR (SCF/STB)	500	900	1386	584	567	1800	450	509	2000
Oil FVF at Bubble Pt	1.285	1.225	1.62	1.283	1.313	2.45	1.284	1.315	1.1 – 1.4
Injection Gas	Air	N_2	CO_2	CO_2	HC	HC	CO_2	HC	HC
Minimum Miscibility Pressure (psi)	--	--	N/A	3334	2131	4640	1900	4257	--
WF recovery (% OOIP)	60	60	60 - 70	N/A	N/A	N/A	N/A	N/A	58
Oil Recovery: (%OOIP)	90.0	> 80.0	60.0	N/A	95.5	84.0	74.8	67.5	N/A

The field reviews show that gas gravity drainage is applicable to all reservoir types and reservoir characteristics using common injectant gases in both secondary as well as tertiary recovery modes. Gravity drainage is 'best applicable' to low connate water, thick, highly dipping or reef type, light oil reservoirs with moderate to high vertical permeability and low re-pressurization requirements. Field applications show oil recoveries as high as 85 – 95% OOIP with calculated average ultimate recoveries for all the fields studied in this review being 76.62% OOIP.

Table 2: Summary of Canadian 'Vertical' HC Miscible Field Applications

Year	Project	Operator	Area (ha)	OOIP MMm^3	Ult. Recovery %OOIP	Dated Prodn %OOIP
1964	Golden Spike D3A Pool	Esso	590	49.60	58.0	56.1
1968	Rainbow Keg River A Pool	Canterra	253	14.30	88.1	61.5
1969	Wizard Lake D3A Unit	Texaco	1075	62.00	95.2	79.9
1969	Rainbow Keg River T Pool	Esso	87	3.18	81.8	55.7
1970	Rainbow Keg River O Pool	Canterra	281	6.21	79.9	61.0
1970	Rainbow Keg River EEE Pool	Canterra	24	1.91	70.2	36.6
1972	Rainbow Keg River E Pool	Canterra	69	3.97	85.4	44.3
1972	Rainbow Keg River G Pool	Canterra	65	2.38	77.3	56.3
1972	Rainbow Keg River AA Pool	Mobil	259	15.90	78.0	40.9
1972	Rainbow Keg River B Pool	Amoco	223	6.52	79.9	50.9
1973	Rainbow Keg River H Pool	Canterra	19	2.35	74.9	59.1
1973	Rainbow Keg River Z Pool	Esso	181	1.49	65.8	44.3
1973	Rainbow Keg River FF Pool	Esso	92	2.50	66.0	41.2
1976	Rainbow Keg River D Pool	Canterra	34	1.13	82.3	53.1
1980	Bigoray Nisku B Pool	Amoco	67	1.50	60.0	28.7
1980	Brazeau River Nisku A Pool	Petro-Canada	108	5.30	75.1	45.5
1980	Brazeau River Nisku E Pool	Petro-Canada	142	2.30	65.1	38.7
1981	Brazeau River Nisku D Pool	Petro-Canada	157	2.70	65.2	28.9
1981	Pembina Nisku G Pool	Texaco	133	3.00	70.0	32.0
1981	Pembina Nisku K Pool	Texaco	58	2.43	70.0	31.7
1981	Westpem Nisku A Pool	Chevron	62	2.65	75.1	34.0
1981	Westpem Nisku D Pool	Chevron	74	2.20	70.0	34.1
1982	Rainbow Keg River B Pool	Canterra	1090	43.00	71.6	43.5
1983	Pembina Nisku M Pool	Canadian Reserve	78	2.85	75.1	27.0
1983	Pembina Nisku O Pool	Texaco	85	1.70	70.0	20.6
1983	Pembina Nisku P Pool	Texaco	170	4.25	75.1	22.4
1983	Rainbow Keg River II Pool	Mobil	73	3.49	75.1	48.7
1984	Rainbow Keg River I Pool	Esso	146	1.88	70.2	N/A
1984	Westpem Nisku C Pool	Chevron	60	4.00	80.0	31.5
1984	Brazeau River Nisku B Pool	Chevron	90	2.30	80.0	29.1
1985	Pembina Nisku A Pool	Chevron	124	2.80	70.0	30.0
1985	Pembina Nisku D Pool	Chevron	143	4.80	72.1	31.7
1985	Pembina Nisku F Pool	Chevron	170	2.10	61.9	3.8
1985	Pembina Nisku L Pool	Texaco	253	5.00	82.0	25.4
1985	Pembina Nisku Q Pool	Texaco	122	2.80	83.9	12.5
1986	Bigoray Nisku F Pool	Chevron	52	2.80	76.1	32.5
1987	Acheson D3 A	Chevron	N/A	3.70	83.8	N/A

3.4 Experimental Design

The original experimental design, fluids used and experimental procedures were described in the previous reports to DOE, 15323R01, (April 2003) and 15323R02 (July 2003). The update and extension of the major project work plan (Figure 4.3.4 of Report 15323R01, (April 2003)) is included in this section.

Firstly, the system behavior (miscible WAG flood) using CO_2-saturated Yates brine shall be investigated. The observed delayed breakthroughs in immiscible CGI floods also need to be studied by conducting secondary waterflood using CO_2-saturated Yates brine, to confirm the hypothesis that in tertiary CGI floods, the unsaturated nature of the brine results in dissolution of the injected CO_2 gas in brine, and consequently making it unavailable for tertiary recovery till the core-fluids become saturated.

Our previous research (Kulkarni, 2003) suggests that for optimum tertiary recovery factors (TRF) and CO_2 utilization factors a 'combination' of CGI and WAG, called the Hybrid-WAG should be employed in miscible floods. Hybrid WAG type corefloods (miscible) need to be conducted using previous TRF maxima in CGI and WAG floods using n-Decane, Yates reservoir brine and pure CO_2.

Tertiary mode GAGD floods are to be conducted using both Berea as well as reservoir cores and actual reservoir fluids to assess their respective performances. Tertiary mode GAGD floods would be performed using both n-Decane + Yates reservoir brine + pure CO_2 and Yates crude oil + Yates reservoir brine + pure CO_2. Minimum miscibility pressure (MMP) between the Yates crude oil and CO_2 should be determined. For justified comparisons, WAG / Hybrid WAG type floods should also be performed at similar conditions.

Oil film flow rates, the parameter dictating ultimate recoveries from gravity stable gas injection projects, are driven by positive spreading coefficients supported in water-wet media, strongly water-wet Berea cores should be used in gravity drainage film flow experiments. Possibility of the use of commercial surfactants, core asphaltene deposition or development of continuous oil-wet paths by making the reservoir mixed wet to promote high film flow rates in reservoirs with different wettability states also should be investigated. The experiments planned for this task are:

n-Decane + Yates Brine + CO_2.

1. Saturated brine tertiary miscible WAG flood.
2. Secondary saturated brine waterflood + tertiary CGI flood.
3. Hybrid WAG flood: Using TRF maxima from CGI & WAG floods.
4. GAGD flood.

Yates Crude + Yates Brine + CO_2.

1. Miscible tertiary WAG.
2. Tertiary CGI flood.
3. Hybrid WAG flood: Using TRF maxima from CGI & WAG floods.
4. GAGD flood.

3.5 Coreflood Results

The core tests were conducted in three steps. The preliminary oil flood was used to measure the connate water saturation of the core. Brine was injected into the core to determine the secondary recovery and residual oil saturation to waterflood. Tertiary gas injection (CGI / WAG / GAGD injection) followed the secondary flood to resemble the sequence of field recovery strategy.

A miscible WAG flood with n-Decane, Yates reservoir brine (previously saturated with CO_2) and pure CO_2 was conducted to compare the results with those using unsaturated Yates brine (included in the previous report to DOE 15323R02 (July 2003)). However, because the brine needs to be saturated with CO_2, precise determination of the CO_2 solubility in the Yates reservoir brine is required for analysis of the coreflood data.

3.5.1 Determination of Solubility of CO_2 in Yates Reservoir Brine

CMG Winprop® was used to determine the solubility of pure CO_2 gas in Yates reservoir brine. The solubility of CO_2 in water was studied as a function of temperature, pressure and salinity. The solubility of CO_2 in fresh water increases with increasing pressure, decreasing temperature (Crawford et al., 1963, Holm, 1963, Jarell, 2002) and the values of CO_2 solubility in fresh water obtained from different experimental studies (Crawford et al., 1963, Holm, 1963, Jarell, 2002) can be adjusted based on the salinity of the brine (at given pressure and temperature) as a percent of solubility retained (Jarell, 2002, Johnson et al., 1952, Martin, 1951, Chang et al., 1996).

The plots obtained form these references were digitized and are plotted below. To facilitate simpler computing procedures, a 6-order polynomial curve was fitted to the experimental data curve used to predict the effect of brine salinity on CO_2 solubility. The experimental data are included as Figure 1 below.

To evaluate and calibrate the simulator with the experimental values, the CO_2 solubility's were calculated at 21.1 ^oC, 37.8 ^oC, 54.4 ^oC, and 87.8 ^oC (70 ^oF, 100 ^oF, 130 ^oF and 190 ^oF) using CMG Winprop®; using two equations of state, viz. Peng Robinson (PR EOS) and Soave Redlich Kwong (SRK EOS) with two viscosity models for water, viz. Jossi-Thiel-Thodos (J-S-T) Correlation and Pedersen Corresponding States Model. The predicted values of solubility at desired conditions (27.8 ^oC (82 ^oF) & 3.4 / 17.2 MPa (500 / 2500 psia)) are summarized in Table 3 and 4 below.

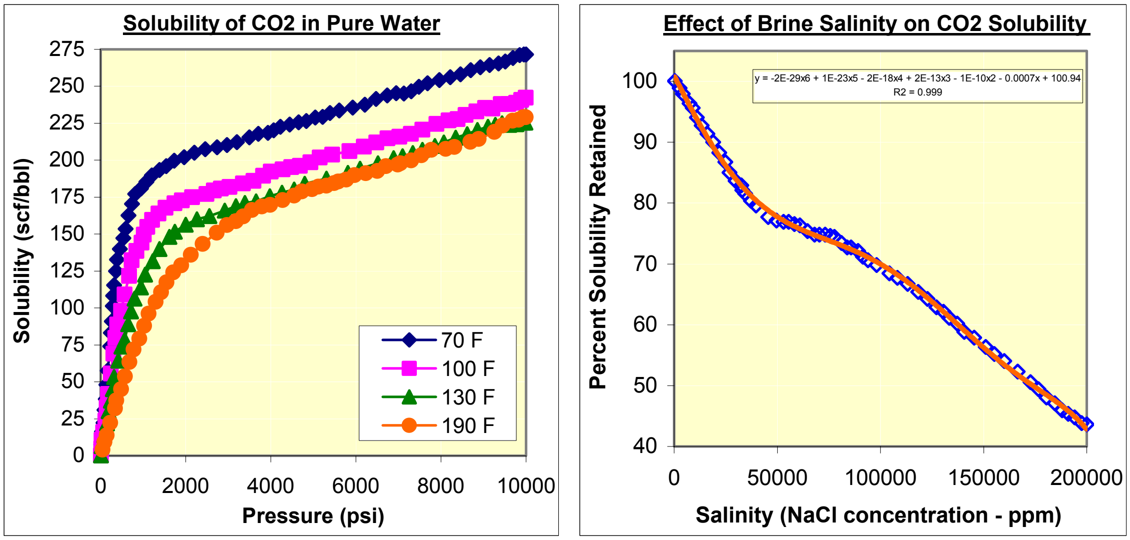

Figure 1: Experimental Solubility Data From Literature (Crawford et al., 1963, Holm, 1963, Jarell, 2002, Johnson et al., 1952, Martin, 1951, Chang et al., 1996).

Table 3: Predicted solubility values at 3.4 MPa (500 psia) & 27.8 C (82 F).

Solubility (mol %)	Data Source
1.89	PR EOS: Adjusted for salinity from pure water simulated value
1.93	SRK EOS: Adjusted for salinity from pure water simulated value
2.27	PR EOS: Brine simulated value
2.29	SRK EOS: Brine simulated value
1.89	Avg. of 21.1 ^{o}C & 37.8 ^{o}C (70 ^{o}F & 100 ^{o}F) data (29.4 C (85 ^{o}F))

Table 4: Predicted solubility values at 17.2 MPa (2500 psia) & 27.8 C (82 F).

Solubility (mol %)	Data Source
3.12	PR EOS: Adjusted for salinity from pure water simulated value
3.32	SRK EOS: Adjusted for salinity from pure water simulated value
3.64	PR EOS: Brine simulated value
3.64	SRK EOS: Brine simulated value
2.84	Avg. of 21.1 ^{o}C & 37.8 ^{o}C (70 F & 100 F) data (29.4 ^{o}C (85 ^{o}F))

Results for 500 psia: The predicted values from simulation for both the EOS show high solubility, than predicted by the experimentally averaged 29.4 ^{o}C (85 ^{o}F) data, as well as that predicted by the adjusted pure water solubility value. The experimental averaged value at 29.4 ^{o}C (85 ^{o}F) is 1.89 mol %, which is close to the prediction of PR EOS (adjusted value). As solubility increases with decreasing temperature, the solubility should be slightly higher than 1.89 mol %. Hence the value of 1.92 mol % predicted by the SRK EOS seems more realistic.

Results for 2500 psia: Solubility increases with decreasing temperature. Hence, the lower predicted solubility value by the 29.4 °C (85 °F) data seems appropriate. Comparison of the simulation data with experimental averaged data (at 29.4 °C (85 °F)) shows that the solubility of 3.64 mol %, as predicted by the PR and SRK simulations, is achievable at pressure > 58.6 MPa (8500 psi). Hence the simulated value of 3.64 mol % seems unrealistic in this case. The averaged data shows that solubility of ~ 3 mol % is obtained at 27.6 MPa (4000 psia) and 29.4 °C (85 °F) range. Therefore, the PR EOS simulated value of 3.12 mol % solubility predicted from adjusting for salinity from pure water data is a good approximation of solubility of CO_2 in Yates reservoir brine.

3.5.2 Miscible WAG Flood In Berea Rock, CO_2-Saturated Yates Brine, and n-Decane System

The flooding sequence consisted of an oil flood (primary drainage), a secondary waterflood (secondary imbibition), and a tertiary gas injection. Rappaport and Leas stability criterion was satisfied in all the floods to avoid flow rate effects.

Oil Flood (Primary Drainage): n-Decane was injected at 160 cc/hr into the core saturated with Yates reservoir brine and drainage from left to right was achieved to establish initial oil saturation. The water recovery and pressure drop behavior are shown as Figure 2 below.

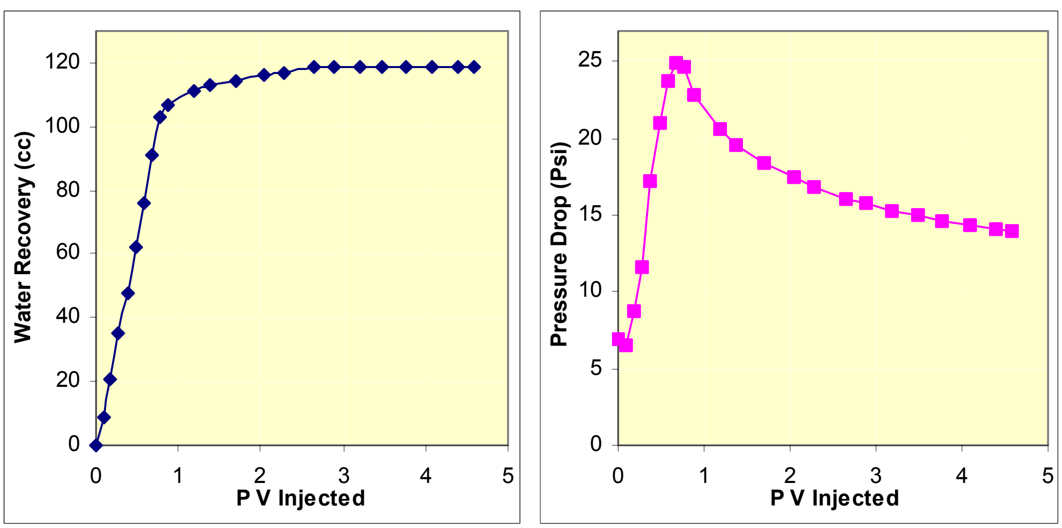

Figure 2: Oil (Drainage) Cycle: Recovery & Pressure Drop Behavior.

The results are comparable to water-wet systems with moderately high connate water saturation (13.3%) and negligible water production after breakthrough with the high end-point oil permeability of 58.3%.

Brine Flood (Secondary Imbibition): The end point permeability of the rock to brine at the end of this cycle can also be used to infer wettability. Yates reservoir brine was injected at 60 cc/hr to establish waterflood residual oil saturation. The oil recovery and pressure drop behavior are shown as Figure 3 below.

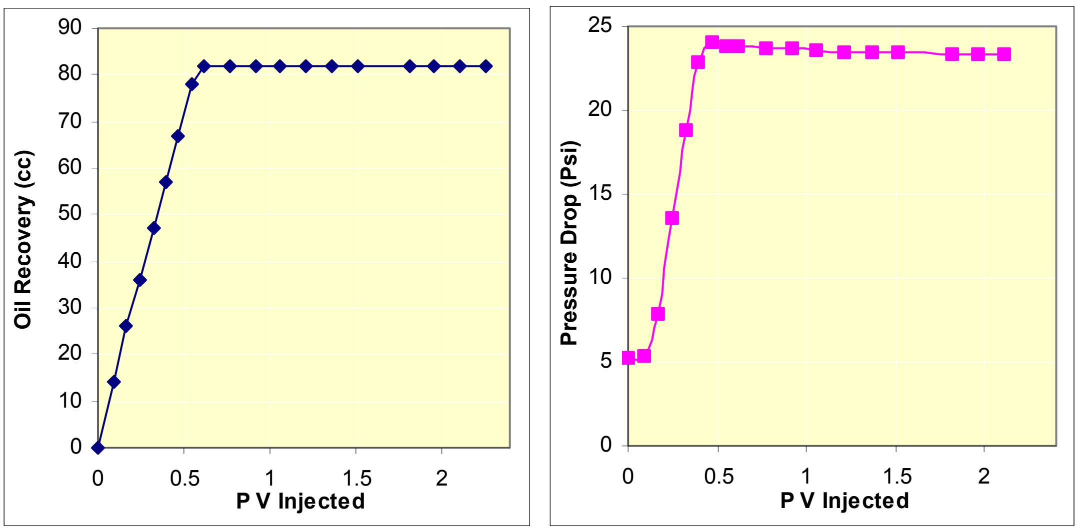

Figure 3: Yates Brine (Imbibition) Cycle: Recovery & Pressure Drop Behavior.

The imbibition results are typical of water-wet cases for the system Higher waterflooding oil recoveries (68.9%), low end point water permeabilities (10.3%), a sharp breakthrough with negligible oil production thereafter as seen in Figure 3, which are all the characteristics of a water-wet rock, were exhibited in the cycle.

Tertiary Gas Injection Flood With Saturated Fluids (EOR - WAG): Pure CO_2 alternating with Yates reservoir brine (saturated with CO_2) was injected into the water-flooded core at 10 cc/hr. The recovery and pressure drop behavior for this cycle is shown in Figure 4 below.

Since the brine was saturated with CO_2, precise determination of the CO_2 solubility in the Yates reservoir brine was required for analysis of the coreflood data. CO_2 solubility in Yates reservoir brine calculation is included in 3.5.1.

Comparison of WAG performance for Saturated & Normal Fluid Floods: The miscible WAG conducted with normal brine fluids was compared with this flood conducted with CO_2-saturated Yates brine. Figures 5, 6 show the comparisons for both floods for water productions, oil productions, pressure drop behavior and TRF plots.

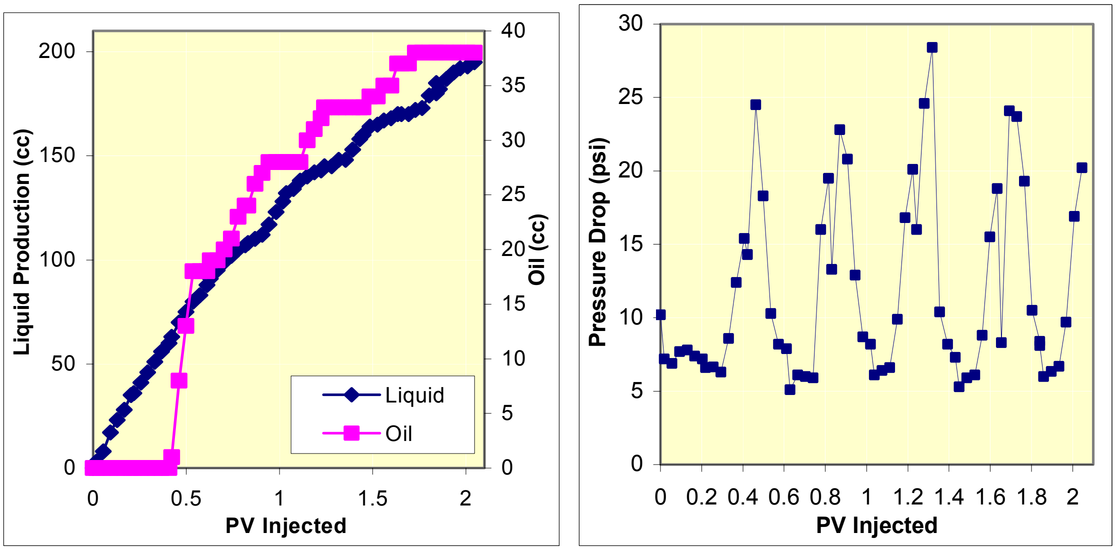

Figure 4: Miscible WAG (Tertiary) Cycle: Recovery & Pressure Drop Behavior

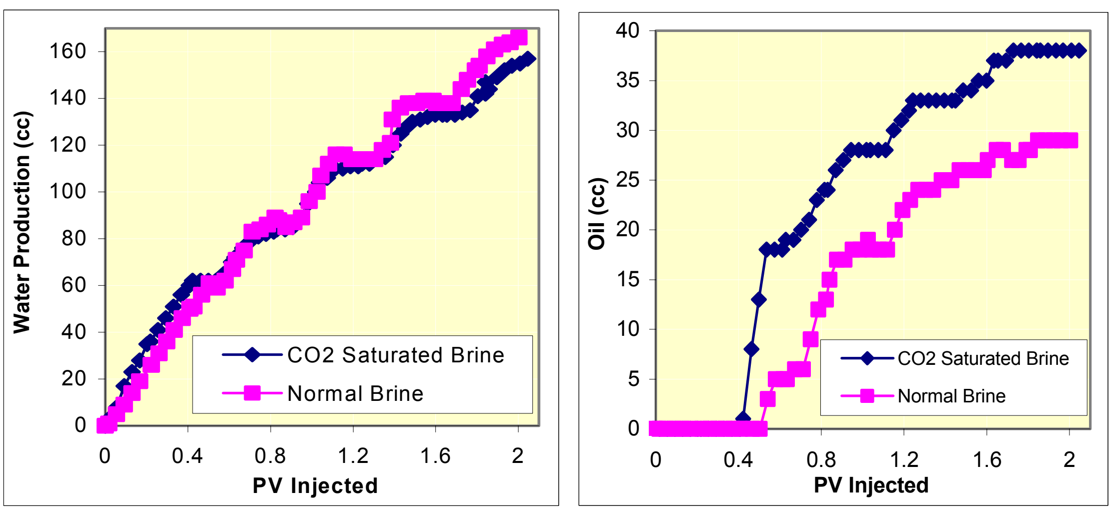

Figure 5: Miscible WAG Floods: Comparison of Water / Oil Productions.

Comparison of the miscible WAG with CO_2-saturated Yates brine (SB Flood) to the normal brine WAG (NB Flood) suggests that:

1. Both floods have identical liquid and water recoveries.
2. SB flood shows significantly higher %ROIP recoveries (89.2%) compared to the NB flood (72.5%).
3. Both floods develop the TRF maxima's are nearly identical pore volume injections (0.84 PVI for NB and 0.82 PVI for NB).

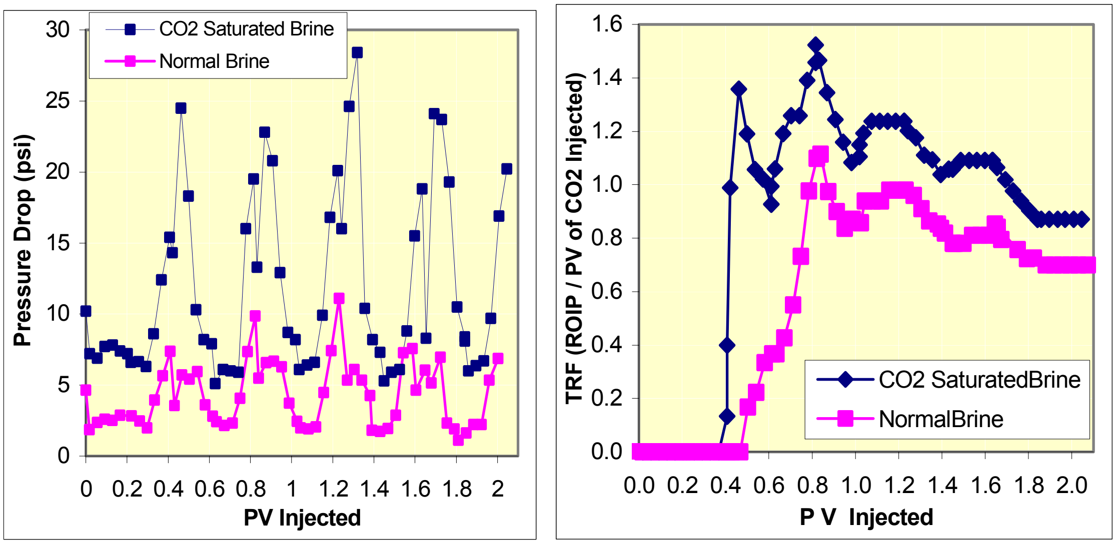

Figure 6: Miscible WAG Floods: Comparison of Pressure Drops and Tertiary Recovery Factors (TRF).

4. SB flood hastens oil breakthrough in the flood (0.47 PVI for NB and 0.37 PVI for NB).
5. Higher gas productions observed in case of SB flood.
6. Increased recoveries in SB flood are attributable to two factors: The decreased tendency of CO_2 to dissolve in core brine – thus resulting in higher available amounts for oil recovery and the improved mobility ratio due to increased viscosity of injected CO_2.
7. However, higher pressure drops are observed in SB floods show: Increased viscous forces in the core, lower gas injectivity as well as lowering of the brine viscosities resulting in decrease in the viscosity contrast between injected fluids.
8. The increased viscosity forces in the reservoir are observed due to the 5.64 times increase of the injected CO_2 viscosity at 2500 psia compared to 500 psia resulting in an average increase of 3.41 times increase in the observed pressure drop. This viscosity increase coupled with higher CO_2 availability for oil recovery results in improved recoveries and TRF's as observed from Figure 6.

To investigate the effect on viscosity of CO_2 solubility in Yates reservoir brine the CMG Winprop® PVT package was used to calculate individual viscosities of CO_2, normal as well as saturated brines from 500 psi to 10,500 psi pressures. Soave Redlich

Kwong equation of state model with Pedersen's corresponding states viscosity model was employed for the calculations. Figure 7 summarizes the results.
The important observations from this simulation study are:

1. Significant increases in CO_2 in-situ viscosities with pressure increase from 500 psia to 1500+ psia.
2. Viscosity increase attributable to above critical CO_2 liquefaction.
3. Systematically lower viscosity of the CO_2-saturated brine than that of normal brine.
4. Improved recoveries of SB flood over the NB flood due to higher CO_2 availability for oil recovery and decreased viscosity contrast of injected CO_2 gas and brine in the core or injected after the CO_2 slug.

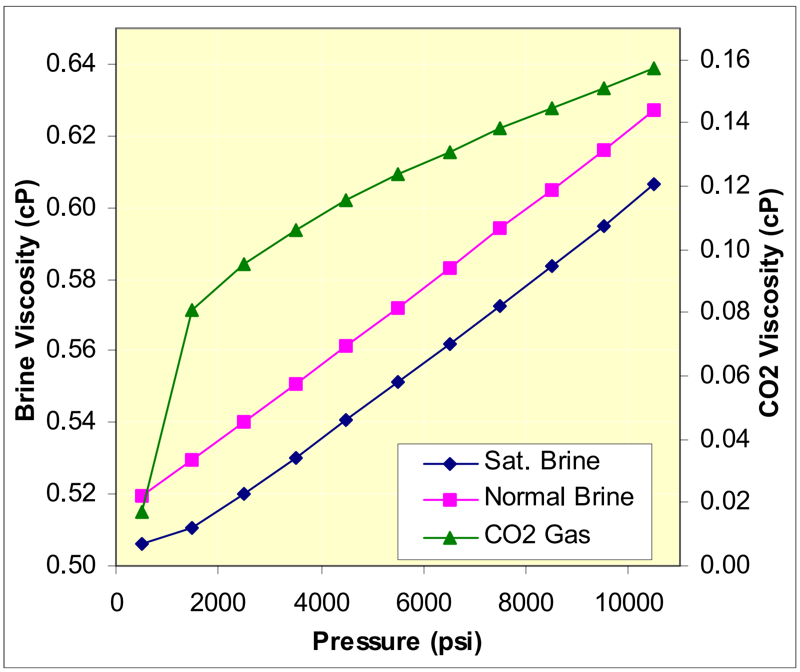

Figure 7: Viscosities of Various Fluids Used for Corefloods.

3.6 Status and Future Work

3.6.1 Status

- A through literature review has been conducted in several research areas related to gas gravity drainage (Included as Appendix 1).
- Simulation studies using CMG Winprop® for determination of experimental fluid properties have been conducted.

- Continued coreflood experimentation with appropriate modifications in the experimental protocol is being conducted.
- Newer findings are being used to define directions of future research.

3.6.2 Future Work

- Continued literature update, focusing on gas gravity drainage of light oil.
- Gravity drainage experiments (GAGD) using the short long cores under different combinations of test conditions.
- ‘Hybrid’-WAG type experiments to determine optimum injection type for CGI and WAG floods.
- Analysis of the preliminary experimental results.
- Use of reservoir fluids in corefloods.

* * *

References

Chang Y B, Coats B K, Nolen J S, "A Compositional Model for CO_2 Floods Including CO_2 Solubility in Water", SPE 35164, Presented at the 1996 Permian Basin Oil and Gas Recovery Conference, Midland, Texas, 27-29 Mar1996.

Crawford H R, Neill G H, Bucy B J, Crawford P B, "Carbon Dioxide A Multipurpose Additive for Effective Well Stimulation", Journal of Petroleum Technology, Mar 1963, pp. 237.

Holm LW, "CO_2 Slug and Carbonated Water Oil Recovery Processes", Producers Monthly, Sept 6, 1963.

Jarrell P M, Fox C E, Stein M H, Webb S L, "Practical Aspects of CO_2 Flooding", SPE Monograph, 2002 pp. 220.

Johnson W E, Macfarlane R M, Breston J N, "Changes in Physical Properties of Bradford Crude Oil When Contacted with CO_2 and Carbonated Water", Producers Monthly, Nov 16, 1952.

Kulkarni, Madhav M, "Immiscible and Miscible Gas-Oil Displacements In Porous Media", MS Thesis, The Craft and Hawkins Department Of Petroleum Engineering, Louisiana State University and A & M College, Baton Rouge, LA, Jul 2003. URL: http://etd.lsu.edu:8085/docs/available/etd-0709103-175151/

Martin J W, "Additional Oil Production Through Flooding with Carbonated Water", Producers Monthly, Jul 18, 1951.

Moritis, G, "Impact of production and development RD&D ranked", Production Editor, Oil and Gas Journal, Oct 30, 1995.Vol 93, Issue 44.

Rao, D N, "Gas Injection EOR – A New Meaning in the New Millennium," JCPT (Feb. 2001) pp. 11-18.

APPENDIX 1: Gravity Drainage Literature Review

A1. Literature Review

Gas Injection Enhanced Oil Recovery (EOR) has become the leading process to recover large amounts of oil left behind in the reservoir by the primary and secondary processes. The world EOR production shows a steep rise in the last two years, with a significant increase of 0.25 MMm^3/d (1.6 MMBbl/d). Gas injection processes, second largest EOR process next to steam processes used in heavy oil reservoirs, produced almost 42% of US-EOR oil in 2002 with the major share of the production from CO_2 injection. The EOR surveys of the Oil and Gas Journal show that the gas injection processes are versatile and were successful in almost all types of reservoirs containing very low to very high waterflood residual saturations.

A1.1 Gas Injection

The gas processes have high microscopic sweep efficiency under miscible conditions; however, the volumetric sweep of the flood has always been a cause of concern (Hinderaker et al., 1996). The mobility ratio, which controls the volumetric sweep, between the injected gas and displaced oil bank in gas processes, is typically highly unfavorable due to the relatively low viscosity of the injected phase. This difference results in severe gravity segregation of fluids in the reservoir.

Gas injection can be considered for four types of applications: WAG, Downdip Injection, Crestal (gas cap) injection, and Gas Recycle mode injection. WAG injection is practiced in normal horizontal reservoirs, where downdip injection is difficult; and the beneficial gravity effects are difficult to obtain. In WAG injection water is alternatively injected with gas to 'offset' or 'mitigate' the gravity segregation phenomenon and achieve a stable flood front (Christensen, 1998). The downdip injection is favored in sloping reservoirs targeting waterflooding residual and attic oil (Jayasekera & Goodyear, 2002). Even in cases miscibility is cannot be achieved there may be benefits from three phase relative permeability effects. WAG type injection can also be practiced for downdip gas injection. Crestal injection is generally useful in saturated reservoirs with gas cap, and gravity stable displacements using miscible or immiscible gas help to increase reservoir sweeps. Crestal type gas injection has been employed on some continental shelves (ex. U.K. Offshore), but this has usually been driven by the need for gas storage or to manage the position of oil rims under gas caps (Jayasekera & Goodyear, 2002). And gas recycle mode process has been proved useful for improved liquid recovery from rich gas condensate reservoirs (Jayasekera & Goodyear, 2002).

Of the above applications of gas injection, the WAG injection is most popular. The WAG process attempts to combine the good microscopic displacement arising from gas injection with improved macroscopic efficiency by injection water to reduce mobility ratio. Hence for improved mobility and flood profile control, water and gas (CO_2 / HC) are alternately injected into the reservoir. The Water-alternating-gas (WAG) process, first proposed by Claudle and Dyes in 1958, is commonly employed to improve the gas injection process performance in the field and today is applied to nearly 83% (49 out of 59 field reviews reported (Christensen, 1998)) of the miscible gas injection field projects. The application of WAG process has yielded better EOR performance than continuous gas injection (CGI) field projects (Kulkarni, 2003).

The best WAG effect is obtained when gravity effects are insignificant, i.e. in reservoirs that are thin or have low permeability (Jayasekera & Goodyear, 2002). However, this expectation may not always be correct, resulting in lower than expected WAG efficiencies. Nevertheless, the attempt to resolve one problem of adverse mobility, the WAG process gives rise to other problems associated with increased water saturation in the reservoir including diminished gas injectivity and increased competition to the flow of oil. This results in severe injectivity problems and difficulties in establishing gas-oil contact and miscibility in the reservoir. The disappointing field performance of WAG floods with oil recoveries in the range of 5 - 10% (Christensen et al., 1998) is a clear indication of these limitations.

Although less popular as an EOR method, the gravity stable crestal or downward displacement type injection, either through gas cap expansion or by gas injection at the crest of the reservoir is an attractive method of oil recovery. The drainage of oil under gravity forces is an efficient method as it can reduce the remaining oil saturation to below that obtained after secondary recovery techniques.

A1.2 Displacement Instabilities for Flow Through Porous Media

Unfavorable mobility contrast is the main reason for the development of instability ‘fingers’ during displacements in porous media. Macroscopic / microscopic heterogeneities result in unequal displacement rates between the displaced and displacing fluid, magnifying the ‘fingering’ phenomenon. Fingers result in poor aerial sweep efficiencies and early breakthrough thus decreasing recovery considerably.

‘Buckley-Leverett’ type displacements are normally difficult to attain mainly due to capillary pressure (immiscible displacements), dispersion effects and poor mobility ratio ($M > 1$) between the displacing and displaced fluids. The instability development is a function of many parameters such as rock and fluid properties, saturation distributions in the porous medium, viscous forces and rock fluid interaction parameters such as wettability, surface tension, development of miscibility etc.

For miscible fluids, Hill (1952) derived a critical velocity expression to predict the rates above which viscous instabilities can occur due to lower gravity compared to viscous forces. The equation, given below, assumed a single interface contact between the injected and displaced phase with no mixing of solvent and oil behind the front.

$$V_C = \frac{2.741.\Delta\rho.k.Sin\theta}{\phi.\Delta\mu} \quad \text{..(1)}$$

Where:

V_C = Critical rate (ft/d)

$\Delta\rho$ = Density difference (gm/cc)

k = Permeability (D)

θ = Dip angle (degrees – measured from horizontal)

ϕ = Porosity (fraction)

$\Delta\mu$ = Viscosity difference (cP)

In 1953, Dietz (1953) proposed a method of analysis of stability of a system with the following assumptions: homogeneous porous medium, vertical equilibrium of oil and water, piston displacement of oil by water, no oil-water capillary pressures, and that the compressibility effects of rock and fluid may be neglected. The Dietz equation is:

$$\tan\beta = \frac{1 - M_e}{M_e.N_{ge}Cos\alpha} + \tan\alpha \text{ ...with } \beta > 0 \text{ being the stability criterion.....................(2)}$$

Where,

M = Mobility Ratio

α = Dip angle

N_{ge} = Gravitational force

Dumore (1964) derived a stability equation, avoiding the limitation of the Hill equation that solvent and oil do not mix. The Dumore equation is given by

$$V_{st} = \frac{2.741.k.Sin\theta}{\phi}\left(\frac{\partial\rho}{\partial\mu}\right)_{\min} \quad \text{..(3)}$$

Where

V_{st} = Critical velocity for stable flow
k = Permeability
θ = Dip angle
ϕ = porosity
$\Delta\rho$ =Density difference
$\Delta\mu$ =Viscosity difference

The Dumore stability criterion is more stringent than the Hill criterion, and for all rates lower than V_{st}; each infinitesimal layer of the mixing zone is stable with respect to each successive layer.

Brigham (1974) observed that the estimate of stability of a coreflood front could be obtained by measuring mixing zone length. The mixing zone length could then be used to calculate the effective mixing coefficient (α_e) an important reservoir simulation parameter. Perkins (1963) and Brigham (1974) solved the diffusion-convection equation and concluded that by measuring the mixing zone between 10% and 90% injected fluid concentrations at the core exit; the effective mixing coefficient (α_e) can be easily determined. Brigham (1974) suggest that in absence of viscous mixing, the effective mixing coefficient (α_e) is a function of the porous medium only and typical values for Berea are 0.001524 m (0.005 ft) in laboratory scale systems.

Rutherford (Used by PRI-ARC) developed a stability criterion for miscible vertically oriented corefloods in laboratory. The equation is given by,

$$(q/A)_{CRITICAL} = 0.0439\frac{k*(\rho_O-\rho_S)}{\mu_O-\mu_S}Sin(\alpha) \qquad (4)$$

Where,
(q/A) = ft/day
k = Darcy
($\Delta\rho$) = lbm/ft3
($\Delta\mu$) = cP
α = Dip angle

Moissis et al. (1987) used numerical simulation techniques to study effects of several parameters on miscible viscous fingering. The important variables considered were the effects of local permeability, overall heterogeneity and mobility ratio. It was found that the local permeability distribution near the entrance of the porous medium plays an important role in finger formation, where as the downstream permeability variations do not significantly affect fingering. The number and growth rates of viscous fingers strongly depend on mobility ratio. The favorable mobility ratios do not generate significant fingers and displacement is uniform in homogeneous porous medium.

Ekrann (1992) generalized the Dietz's correlation to establish a stability criterion in stratified reservoirs. Virnovsky et al. (1996) used analytical and numerical techniques to study the stability oil-gas-water displacements in two spatial dimensions. It was concluded that stable oil-gas-water displacement fronts, if at all occur, they do so only for a limited number of injection gas-water ratios. The authors argue that this stability analysis is applicable to more practical applications like WAG, and suggest the optimization of the WAG ratio based on this stability analysis.

Coning is another serious production problem in gas injection projects. Coning and displacement stabilities are considered different production issues (Supraniowicz & Butler, 1989). However, coning problems are attributed to the mobility contrasts in displacements, and can occur in both water-drive and gas-drive type displacements. The stability criterion applicable, discussed in the previous section, to viscous instabilities is not necessarily applicable to coning problems and critical velocity constraints to mitigate coning are generally stricter. With the use of horizontal wells in gravity drainage applications becoming popular, most of the analysis available in this field deals with the production from horizontal wells with vertical injectors.

A1.3 Critical Rates for Gravity Drainage

Slobod and Howlett (1964) derived a critical rate equation for frontal stability in homogeneous sand packs and is given by –

$$q_{oc} = \frac{k_o}{\Delta\mu_o}.(\Delta\rho.g) \qquad (5)$$

Barkve and Firoozabadi (1992) derived the initial (also maximum) gravity drainage rate (q_o) for an immiscible process in a homogeneous rock matrix is given by –

$$q_o = \frac{k_o}{\mu_o}.(\Delta\rho.g - P_c^{(TH)} / L) \qquad (6)$$

Where:
k_o = Single phase oil permeability
μ_o = Oil viscosity

$\Delta\rho$ = Density difference between injected / displaced fluids
g = gravitational acceleration
$P_c^{(TH)}$ = Threshold capillary pressure
L = Height.

The assumptions in the derivation included infinite gas mobility during displacement. The authors also comment that in the initial phase, the gravity drainage rate in fractured media does not exceed the un-fractured media, provided the fractures have negligible storage. In developed flow conditions, the capillary pressure contrast between the matrix and fracture, results in lower gravity drainage rates in case of fractured media.

For miscible displacements (capillary pressure = 0), the initial (also maximum) gravity drainage rate (q_o) in a homogeneous rock matrix is given by –

$$q_o = \frac{k_o}{\mu_o}.(\Delta\rho.g) \qquad \text{.......(7)}$$

Comparison of the two equations (5 & 7) shows that the maximum drainage rate (q_o) is less than critical rate (q_{oc}) when the displacing fluid has a negligible viscosity (e.g. gas displacement).

Supranowicz and Butler (1989) examined the vertically confined waterflood to horizontal wells assuming equal water / oil densities. The authors define a critical production rate equation beyond which fingering would occur. This critical rate is different than for coning / cresting and authors considered it 'a serious limitation' in horizontal wells. It is suggested that this analysis be used to constitute production rate guidelines in the horizontal producers to prevent fingering and coning problems.

Meszaros et al. (1990) examine the potential use of inert gas injection using horizontal wells using scaled model studies and numerical simulation. Johnson scaling criterion was used for the physical models. The authors suggest that for high recovery factors the stability of the displacing front is important, and that a slant / horizontal front propagation results in severe reduction in recoveries.

Butler (1992) presents the theoretical analysis for production from heavy oil reservoirs via gravity drainage with a gas cap advancing downward a horizontal well. It was assumed that the reservoir pressure is maintained by crestal gas injection and production rate is controlled to just below the critical rate for gas coning. It was assumed that there is vertical fluid flow in the vicinity of the horizontal well. The potential gradient extending along vertical plane extending through the horizontal well located at the base of the reservoir.

The straight line corresponds to simple radial flow from an unbound reservoir and is given by –

$$\Phi = \frac{2.q.\mu}{\pi.k.L}.\ln(y) \text{ ....One Side...(8)}$$

Where
q = Oil production rate to vertical well from one side of horizontal well
k = permeability
L = Length of horizontal well
μ = Viscosity
y = Height of interface
Φ = Potential

Whereas the curved line depicts the reservoir confined by two vertical boundaries as derived by Maxwell as well as Muskat. The potential equation is given by –

$$\Phi = \frac{2.q.\mu}{\pi.k.L}.\ln\left[\cosh(\frac{\pi.y}{W}) - \cos(\frac{\pi.x}{W})\right] \text{ ....(9)}$$

$$\Phi_{(x=0)} = \frac{2.q.\mu}{\pi.k.L}.\ln\left[\cosh(\frac{\pi.y}{W}) - 1\right] \text{ ....One Side...(10)}$$

Where
q = Oil production rate to vertical well from one side of horizontal well
k = permeability
L = Length of horizontal well
μ = Viscosity
y = Height of interface
Φ = Potential
W = Horizontal distance from horizontal well

Thus, in the near well-bore region (of a horizontal producer), the two equations result in the same potential gradient, while far above the well, the potential gradient becomes constant and results in linear flow between parallel boundaries. It was also assumed that for critical flow, the potential gradient in the liquid interface above the well, at height h_W, can be calculated using the above equation, and it must equal ($\Delta\rho.g$) for critical flow.

Butler (1992) notes that for very small well spacing, the critical flow is determined by the tendency for interfacial instability in a simple flat interface moving downward (drained horizontal fracture). On the other hand, for large well spacing, the critical production rate is dictated by the need for horizontal displacement of oils as against the vertical limitation for very small well spacing, which is intuitive. The authors explain that for most practical cases, the 'conventional' well spacing is larger than the maximum limit set by this theory, and considerable improvements in well productivity can be achieved by decreasing the well spacing.

A1.4 Laboratory Studies for Gravity Drainage

Green and Willhite (1998) suggest that the same density difference that causes problems like poor sweep efficiencies and gravity override in these types of processes can be used as an advantage in dipping reservoirs. The beneficial results of flooding in gravity stable mode have been demonstrated by many laboratory and field studies.

Gravity-assisted displacements offer the advantages of eliminating gravity tongues and stabilizing viscous fingers. Tiffin and Kremesec (1986) conducted a series of gravity-assisted vertical core displacements of both first contact miscible and multiple contact miscible type, with CO_2 – recombined crude oil systems at various pressures and temperatures. Significant improvements of the vertical flood performance over similar horizontal core displacements were observed. In an attempt to elucidate the mechanisms of the process, the authors that while miscibility development in vertical core displacements was at similar pressures as their horizontal counterparts, miscibility was achieved in the vertical downward displacement at a considerably shorter core length. The paper also demonstrates that component mass transfer, similar to those in multiple contact miscible processes, strongly affect flood front stability and that displacement efficiency increases at lower fluid cross flow and mixing conditions.

Kantzas et al. (1988) analyzed the mechanisms in gravity drainage processes by measuring capillary pressure curves for capillaries of regular pore geometry. The analysis was done for immiscible fluid and water-wet rock systems, and a pore co-existence criterion for three immiscible phases was defined to determine water and oil saturation distributions at pore level.

Chatzis et al. (1988) carried out downward displacements of oil by injection of inert gas at initial and waterflood residual oil saturations. Very high recovery efficiencies under strongly water-wet systems in consolidated or unconsolidated porous media were observed. Further experimentation with CT scans and regular capillary tubes for immiscible gravity stable inert gas displacements conclude that very high recoveries under these conditions are only possible when oil spreads over water, the reservoir is strongly water wet and a continuous film of oil over the water in the corners of the pores invaded by gas exists. The spontaneous spreading of oil at the water gas interface is limited in the case of water wet rock samples and positive spreading coefficients.

CO_2 cyclic 'huff and puff' injection in Berea cores using live oil samples for gravity stable (vertical) displacements and dead oil samples with horizontal cores were studied by Thomas et al. (1990). It was found that gas cap, gravity segregation as well as higher residual oil saturations help to increase the overall oil recovery in gravity-stable floods. Moreover, it was observed that gravity segregation (beneficial in gravity-stable floods) helps deeper penetration of CO_2 (hence better recovery), and accidental injection of CO_2 in gas cap do not have detrimental effects on recovery.

Mungan (1991) conducted miscible and immiscible coreflood experiments using heavy and light oils with CO_2. It was concluded that CO_2 could increase heavy oil recovery even without miscibility development. Furthermore breakthrough recovery increase from 30% to 54% was observed when CO_2 was used instead of CH_4 as a displacing fluid.

Karim et al. (1992), similar to Thomas et al. (1990), conducted CO_2 cyclic 'huff and puff' coreflooding experiments using 6-ft long Berea cores and Timbalier Bay light crude. The core-inclination was found to substantially influence the oil recovery efficiencies and gas utilization factors of the coreflood and the 'best' performance was observed when CO_2 was injected into the lower end of a core tilted at a 45 or 90 degree angle.

Oren et al. (1992) attempted to characterize the pore-scale displacement mechanisms responsible for mobilization and production of waterflood residual oil accountable to immiscible gas flooding. A numerical three-phase invasion-percolation type network model was built incorporating these pore-scale displacement mechanisms, and used to predict the recoveries due to tertiary mode gas floods for 3-phase water-wet type systems with varying spreading coefficients. The model concluded that spreading oil films (i.e. positive spreading coefficients) are important to increase tertiary waterflood residual oil recovery by gas injection.

Kalaydjian et al. (1993) conducted sand-pack experiments in both horizontal and gravity stable modes. These results were similar to the previous experimental findings that the gravity stable floods had higher incremental recoveries over horizontal floods.

Longeron et al. (1994) studied the influence of capillary pressure on oil recovery. It was shown that the gas-oil capillary pressures were always higher in presence of connate water than the capillary pressures without connate water saturation. Further investigation using numerical simulation showed that recovery was very sensitive to capillary pressure input data, and the authors suggest “using scaled capillary pressures from mercury-air data, the recovery is underestimated by about 6% PV”.

Chalier et al. (1995) used the gamma-ray absorption technique to visualize the fluid saturation distribution in the core as a function of the volume of gas injected. The three-phase oil relative permeability curve was analytically deduced from the oil saturation profiles and used for development of a numerical triphasic relative permeability model. The authors emphasize “three-phase oil relative permeability was the key for the evaluation of tertiary gas-gravity drainage project”.

The above laboratory studies show that residual oil saturation, oil relative permeability and three-phase flow conditions not only are dependant on wettability of the porous medium but also are strongly influenced by the spreading coefficient. A positive spreading coefficient is desirable for continuous oil films on water and result in higher oil recovery factors in strongly water-wet systems.

A1.5 Field Studies of Gravity Drainage

The gravity drainage process has been applied and has been successfully implemented in many field applications and pilots. Coreflood as well as field studies (Lepski and Bassiouni, 1998) have confirmed that incremental oil could be recovered from dipping water-drive reservoirs using gravity assisted gas injection processes such as Double Displacement Process (DDP), and Second Contact Water Displacement (SCWD).

Empirical screening criteria for gravity assisted gas injection are available in the literature (Lepski and Bassiouni, 1998) and are summarized below as Table 5.

Table 5: Screening Criteria For Gravity Assisted Gas Injection.

Parameter	Value
WF Residual Oil Saturation	Substantial
Reservoir Permeability	> 300 mD

Bed Dip Angle	> 10^o
Oil Viscosity	Free flow
Spreading Coefficient	Positive

King and Lee (1976) developed modeling techniques to study the Hawkins (Woodbine) field in East Texas. Reservoir characterization was done using 10942.3 m (35,900 ft) of conventional cores obtained from 193 wells in the field. The field oil gravity varied from 12 to 30 API with viscosity varying from 2-80 cP. The reservoir characteristics include 40468730 m^2 (10,000 acres) of area with > 304.8 m (1000 ft) of hydrocarbon column. The reservoir is highly faulted with 6^o dip with strong aquifer support. Detailed phase behavior and modeling studies suggested gas injection to prevent oil encroachment in the gas cap and prevent further shrinking. Predictive simulation studies indicated that ~ 30.1 million m^3 (189 million bbl) of additional oil could be produced of which 18.4 million m^3 (116 million bbl) would be produced by converting the water-drive areas into gas-drive/gravity drainage, and 10.7 million m^3 (67 million bbl) from prevention of the oil loss caused by gas cap shrinkage. The authors conclude that the gas-drive/gravity drainage process would help produce nearly 33% more oil than possible through water drive.

DesBrisay et al. (1981) reviewed the vertical gravity stable miscible flood performance in the Intisar 'D' reservoir in the Libyan Sirte basin. Geologic studies show the reservoir as upper Paleocene pinnacle reef, roughly circular (diameter 4828.0 m (~ 3 miles)) in plan with original hydrocarbon column of 289.6 m (950 ft). The reservoir oil was highly under saturated, very light (40^o API) with 0.46 cP viscosity. The calculated MMP of this oil with gas in nearby fields (27.6 MPa (4000 psi)) was lower than the original reservoir pressure of 29.4 MPa (4257 psi). Modeling studies showed that the volumetric nature of the reservoir would result in extremely low primary recoveries, and pressure maintenance program by both water injection and crestal gas injection was initiated. "Extensive reservoir engineering studies indicated that miscible gas injection would almost double the waterflood oil recovery and would also conserve large amounts of solutions gas being produced from this and other fields". The authors predict that almost 0.25 billion m^3 (1.6 billion bbl) of OOIP (of which 78.9 million m^3 (496 million bbl) recovered till date) would be recovered yielding a recovery factor of ~ 70%, and most of which is attributable to miscible gas gravity drainage.

Cardenas et al. (1981) presented a laboratory design for a gravity stable miscible CO_2 flood for the Texaco's Bay St. Elaine field, Terrebonne parish, LA. The reservoir oil characteristics include light (36 ^{o}API) oil and viscosity 0.667 cP, with 20% residual waterflood oil saturation, with an MMP of 22.9 MPa (3334 psi) with CO_2 gas which was the current reservoir pressure. The reservoir had a 36^o dip and is well confined with natural sealing faults. The paper describes the following studies that were conducted:

PVT studies

Empirical design of CO_2 solvent slug

The critical velocity for gravity stable flooding was calculated using a modified Dumore (Dumore, 1964) equation shown below,

$$V_C = 8.473E-04.\frac{K_m.Sin\alpha_d(\rho_2-\rho_1)}{\phi_m(\mu_2-\mu_1)} \quad \text{(11)}$$

Where,
V_C = Critical front velocity (m/day),
K_m = Mobile fluid permeability (μm^2)
α_d = Angle of dip (degrees)
ρ = Fluid density (kg/m^3). 1 = displacing, 2 = displaced
ϕ_m = Mobile fluid porosity
μ = Fluid viscosity (m-Pa-s). 1 = displacing, 2 = displaced

Reduction in the density of CO_2 slug by addition of CH_4 gas to ensure gravity stable and miscible displacement was done after the study.

Slim tube tests

Based on the results of PVT analysis, four CO_2-solvent mixtures were prepared using pure components. Displacement tests using these four solvent mixtures were conducted using 12.2 m (40 ft) & 0.006 m (¼") ID SS slim tube packed with clean silica sand. The slim tube results indicated an MMP of 22.9 MPa (3334 psi).

Sand Pack floods

Two 1.9 m (6 ft) & 0.06 m (2.5") ID sand packs filled with clean silica sands (2400 mD and 36% porosity) were used to study two types of displacements: Continuous slug injection and CO_2 slug followed by N_2 chase gas. The slug flood exhibited a residual oil saturation of 5.8% while the continuous flood had a residual oil saturation of 4.1%.

The analysis indicated a 0.24 PV CO_2 slug would be required for the field project, however to provide an adequate safety factor to account for losses and ensure better oil recovery a 0.33 PV slug was selected for the Bay St. Elaine CO_2 project. However, field performance was not reported.

Nute (1983) evaluated the miscible Bay St. Elaine Field flood performance using pulse pressure tests, and measurements of oil saturations in situ to improve reservoir definition. The author describes the flood as 'successful' however production data are not available.

Backmeyer et al. (1984) reported the tertiary extension of the Wizard Lake D3A pool, Alberta, HC miscible flood and updated the secondary flood data. The reservoir is dolomitized bioherm reef of Devonian age with oil zone of 197.5 m (648 ft) with a bottom water drive (Cooking Lake aquifer). The reservoir characteristics include vuggular and matrix porosities with average horizontal permeability of 1375 mD and average vertical permeability of 107 mD with original reservoir pressure of 15.7 MPa (2270 psi). Reservoir oil is paraffin based 38 ^{o}API crude with saturation pressure of 14.7 MPa (2131 psi) at 71.1 ^{o}C (160 ^{o}F). The secondary HC miscible slug injection was 7.5% HCPV, and with the extension of the HC miscible flood in the Wizard Lake D3A pool – tertiary block, the projected recovery increase was 4.5 MMm^3 (28.5 MMSTB) thus raising the overall recovery from the reservoir to 59.3 MMm^3 (372.7 MMSTB) or 95.5% overall recovery factor.

Johnston (1988) summarized the Weeks Island S sand reservoir B (S RB) gravity stable field test. The S RB reservoir was chosen due to the small, well confined nature and exceptional sand quality and continuity. Reservoir characteristics include permeability of 1200 mD and a bed dip of 26^{o}.The reservoir oil properties are not specified, however residual oil saturation before the pilot was 22% based on SCAL. Low oil rates, water cuts and increasing GOR made tertiary recovery (CO_2 injection) necessary in the field. A 25.5% PV gravity stable miscible CO_2 – HC slug (24% PV & 1.5% PV) was injected resulting in additional 32.5924 Mm^3 (205 MBbl) or 60% waterflood unrecoverable oil. The displacement efficiencies were found > 90% (sidewall cores) and a CO_2 usage rate of 1407.05 m^3/m^3 (7.90 MCF/bbl) considering the recycled gas.

Howes (1988) summarized the EOR projects in Canada till date. There were 51 commercial scale projects (all hydrocarbon (HC) miscible) operational in Canada for recovery of light – to- medium crude (Density < 900 kg/m^3) and the gravity stable 'vertical' floods conducted in Canada till 1986/12/31 are compiled in Table 6 below. Detailed description and analysis of the projects are un-available and out of scope of the study.

The comparisons of the projects showed that oil recoveries were much higher, in the range of 15 – 40 % OOIP, for gravity stable gas floods in the pinnacle reefs of

Alberta, compared to WAG recoveries of 5 – 10 % (Christensen et al., 1998). The miscible flood average ultimate recovery factors in Alberta were 59% OOIP, whereas the Alberta waterflood ultimate recoveries were only 32%.

Table 6: Summary of Canadian 'Vertical' HC Miscible Field Applications.

Year	Project	Operator	Area (ha)	OOIP MMm^3	Ult. Recovery %OOIP	Dated Prodn %OOIP
1964	Golden Spike D3A Pool	Esso	590	49.60	58.0	56.1
1968	Rainbow Keg River A Pool	Canterra	253	14.30	88.1	61.5
1969	Wizard Lake D3A Unit	Texaco	1075	62.00	95.2	79.9
1969	Rainbow Keg River T Pool	Esso	87	3.18	81.8	55.7
1970	Rainbow Keg River O Pool	Canterra	281	6.21	79.9	61.0
1970	Rainbow Keg River EEE Pool	Canterra	24	1.91	70.2	36.6
1972	Rainbow Keg River E Pool	Canterra	69	3.97	85.4	44.3
1972	Rainbow Keg River G Pool	Canterra	65	2.38	77.3	56.3
1972	Rainbow Keg River AA Pool	Mobil	259	15.90	78.0	40.9
1972	Rainbow Keg River B Pool	Amoco	223	6.52	79.9	50.9
1973	Rainbow Keg River H Pool	Canterra	19	2.35	74.9	59.1
1973	Rainbow Keg River Z Pool	Esso	181	1.49	65.8	44.3
1973	Rainbow Keg River FF Pool	Esso	92	2.50	66.0	41.2
1976	Rainbow Keg River D Pool	Canterra	34	1.13	82.3	53.1
1980	Bigoray Nisku B Pool	Amoco	67	1.50	60.0	28.7
1980	Brazeau River Nisku A Pool	Petro-Canada	108	5.30	75.1	45.5
1980	Brazeau River Nisku E Pool	Petro-Canada	142	2.30	65.1	38.7
1981	Brazeau River Nisku D Pool	Petro-Canada	157	2.70	65.2	28.9
1981	Pembina Nisku G Pool	Texaco	133	3.00	70.0	32.0
1981	Pembina Nisku K Pool	Texaco	58	2.43	70.0	31.7
1981	Westpem Nisku A Pool	Chevron	62	2.65	75.1	34.0
1981	Westpem Nisku D Pool	Chevron	74	2.20	70.0	34.1
1982	Rainbow Keg River B Pool	Canterra	1090	43.00	71.6	43.5
1983	Pembina Nisku M Pool	Canadian Reserve	78	2.85	75.1	27.0
1983	Pembina Nisku O Pool	Texaco	85	1.70	70.0	20.6
1983	Pembina Nisku P Pool	Texaco	170	4.25	75.1	22.4
1983	Rainbow Keg River II Pool	Mobil	73	3.49	75.1	48.7
1984	Rainbow Keg River I Pool	Esso	146	1.88	70.2	N/A
1984	Westpem Nisku C Pool	Chevron	60	4.00	80.0	31.5
1984	Brazeau River Nisku B Pool	Chevron	90	2.30	80.0	29.1
1985	Pembina Nisku A Pool	Chevron	124	2.80	70.0	30.0
1985	Pembina Nisku D Pool	Chevron	143	4.80	72.1	31.7
1985	Pembina Nisku F Pool	Chevron	170	2.10	61.9	3.8
1985	Pembina Nisku L Pool	Texaco	253	5.00	82.0	25.4
1985	Pembina Nisku Q Pool	Texaco	122	2.80	83.9	12.5
1986	Bigoray Nisku F Pool	Chevron	52	2.80	76.1	32.5
1987	Acheson D3 A	Chevron	N/A	3.70	83.8	N/A

Texaco's Wizard Lake D-3A pool reservoir, Alberta was under primary production since 1951, history of which 19 years had primary production and nearly 20 years of gravity stable HC miscible injection. Hsu (1988) developed a 3-D (11 x 14 x 53), 4-phase (gas, solvent, oil & water) simulation model to predict reservoir behavior so as to help plan better injection-production strategy for the reservoir. The central theme of the paper was the good history match for ~ 40 years of reservoir production and model features developed specifically for this reservoir case.

Laboratory studies for the performance evaluation of the Hawkins field, under gas drive – pressure maintenance, were studied by Carlson (1988). It was concluded that the gas gravity drainage process had a recovery efficiency of > 80% compared to the water drive efficiency of only 60%. It was concluded that even under immiscible conditions, the gas could recover additional oil from the water invaded portions of the reservoir and thereby reducing the residual oil saturation in water invaded oil column from 35% to about 12%. The above conclusion helped the development of the 'Double Displacement Process' (DDP) and initiation of a field DDP pilot in the east fault block of the reservoir. The pilot test results are not included.

Da Sle and Guo (1990) analyzed the vertical hydrocarbon miscible flood in Westpem Nisku D pool, 160934.4 m (100 mi) southwest of Edmonton, Canada. The reservoir was of pinnacle reef type and the miscible flood implemented in May 1981 with a miscible slug of 80% Methane and rest of C_{2+} fraction, which was later changed to 85% C1, and 15% C_{2+} fraction with 33.1 MPa (4800 psi) working pressure to assure miscibility development. The reservoir oil was light (45 API) with 0.19 cP viscosity. Flood analysis for solvent/oil interface behavior showed that the interface was consistently flat across the reef, as predicted by the Dumore stability criterion. Further the core-analysis results indicated very low residual oil saturation to the order of 5% making the flood a success.

Bangla et al. (1991) studied the field performance of the gravity stable vertical CO_2 flood in Wellman unit of the Wolfcamp reef reservoir, which is a limestone reef reservoir in western Midland basin of Terry county, Texas. Reservoir oil was light (43.5 API) with 0.43 cP viscosity. A tertiary CO_2 miscible flood was planned after a successful waterflood with a ROS of 35%. CO_2 was injected into crest of reservoir with water injection continued in the water zone to maintain the MMP of 13.1 MPa (1900 psi). Numerical model was constructed previously to predict the performance of the CO_2 injection under gravity stable modes. The model predicted the CO_2 ultimate sweep efficiency to be 78%. The actual sweep efficiency was found better than expected at 84% and the critical residual oil saturation was only 10.5% compared to the waterflood residual of 35%. The net utilization ratio of the flood was 1157.7 m^3/m^3 (6.5 MSCF/STB) and the ultimate recovery was 68.8% of the OOIP of the field with CO_2 incremental recovery of 27% excluding 'sandwich loss'. Further developments suggested may push the ultimate recovery up to 74.8% of the OOIP. The wettability of the reservoir rock is not mentioned; nevertheless, the CO_2 miscible project was highly successful.

Huge reservoirs such as the Prudhoe Bay may have many oil recovery mechanisms operational in the field. For proper field management, understanding of the interaction / interdependence of these recovery mechanisms is critical. One of the common mechanisms operational, not only in Prudhoe Bay but many reservoirs where gravity drainage is the dominant production mechanism, are gravity drainage and bottom water drive or waterflood. Espie et al. (1994) tried to quantify these mechanisms via core studies and numerical simulation techniques. Espie et al. (1994) conducted series of corefloods using Prudhoe Bay cores and Prudhoe Bay analogue fluids at ambient conditions with the intention of mechanistic investigation of three phase flow. The flood sequence was:

Waterflood

Tertiary displacement I

Gas / Oil gravity drainage from initial water saturations followed by waterflood.

Tertiary displacement II

Gas / Oil gravity drainage experiment from initial water saturations followed by an injected oil slug then followed by waterflood.

It was found that the initial oil saturation, oil mobility, and trapped gas saturation were critical to determine the velocity of the oil bank and that either the Stone I and Cheshire 3-phase relative permeability models could predict the 1D experiment efficiently.

Durandeau et al. (1995) studied the application and integration of the new sponge coring technology to obtain the fluid distributions and efficiency of the gas gravity drainage floods in one of the Arab D sub-reservoirs of a major oil field in offshore Abu Dhabi. SCAL and centrifuge tests were conducted on the cores to determine effective oil saturations. The authors quote: "The effective oil saturation results showed that the gravity segregation mechanism has been very active and efficient to recover the oil in the reservoir". However detailed data to support this statement is not available in the paper.

Langenberg et al. (1995) documented initial 6 years of the double displacement process (DDP) in the East fault block 'Dexter' sands of the Hawkins Field, Wood county, Texas. Field histories showed that the field, producing under strong bottom water drive, resulted in the invasion of the oil columns into the gas cap. To reduce further gas cap shrinkage; inert gas (N_2) shrinkage was started in March 1977. Studies showed that the gravity drainage rate was lower than expected and hence the injection rates were revised using Richardson-Blackwell gravity drainage rate calculations. The authors suggest that the DDP process has been successful in EFB and can reduce the residual oil saturations substantially thus improving recovery considerably.

Fong et al. (1999) compile the design factors and operational strategies for a successful tertiary 'vertical' miscible flood scheme and present their application to a tertiary hydrocarbon miscible flood in the NW lobe of the Rainbow Keg River F Pool reservoir. The authors suggest that the successful design factors are:

1. Operating pressure selection
2. Optimal solvent composition to ensure first contact miscible (FCM) displacement, there by reducing technical risks associated with miscibility, dispersion, diffusion and gravity stabilization.
3. Optimum solvent size to maintain miscibility throughout the life of flood as well as prevent loss of miscibility by accidental mixing and dispersion with chase gas.
4. Critical frontal advancement rate should be greater than vertical advancement rate (Dumore stability criterion applied).
5. Good pattern design to ensure proper placement of solvent slug.

Field performance monitoring showed significant oil production improvement in the early life of the flood, attributable to the high reservoir quality, proper design criteria and sound operational strategy.

Gunawan and Caie (1999) analyzed the Handil reservoir performance for three years of lean gas injection in the Mahakam delta of Borneo, Indonesia. Reservoir and economic studies showed that the crestal injection of lean HC gas into the water flooded Handil field would yield additional oil from this near abandonment reservoir. Predictive simulation studies predict that the reservoir would yield additional 4.8 MMm^3 (30 MMSTB) EOR oil.

Ren et al. (2003) used IMEX® black oil simulator to study the macroscopic level mechanisms of the DDP process. The 3D model was populated using reservoir properties from successful tertiary gas gravity drainage field tests. The important conclusions are:

1. Injection/production rates strongly affect oil bank formation and recovery.
2. Highly dipping reservoirs are good candidates for gravity assisted tertiary gas injection.

3. Accurate modeling of 3-ϕ relative permeability and capillary pressures is necessary for accurate representation of the process.
4. The secondary contact water displacement process (SCWD) fares better than DDP since higher oil drainage rates are obtained.

The incremental oil obtained in the gravity assisted tertiary gas injection processes is twofold –

Recovery of the bypassed oil

Recovery of continuous oil phase that was unrecoverable in previous processes on account of reservoir heterogeneity and well placement.

Recovery of residual oil in water swept zones

Discontinuous oil phase trapped due to capillary and viscous forces.

The positive spreading coefficient helps the formation of oil films in the pores when it comes in contact of the gas. These films can connect to all the residual oil in the gas swept zone to the oil bank in front of the gas front. Thus incremental oil recovery is due to oil film flow, and hence the rate of oil recovery is a strong function of the rate of oil drainage through these oil films.

The summary of the above cited field applications are included in Table 7 below for ready reference.

Table 7: Summary of above cited Gravity Drainage Field Applications.

Property	West Hackberry	Hawkins Dexter Sand	Weeks Island S RB - Pilot	Bay St. Elaine	Wizard Lake D3A	Westpem Nisku D	Wolfcamp Reef	Intisar D	Handil Main Zone
State / Country	LA	Texas	LA	LA	Alta	Alta	TX	Libya	Borneo
Rock Type	Sand-Stone	Sand-stone	Sand-stone	Shly-Sand	Dol-omite	Carb-onate	Lime-Stone	Biomicrite/Dolo.	Sand-stone
Porosity (%)	27.6 – 23.9	27	26	32.9	10.94	12	8.5	22	25
Permeability (mD)	300 – 1000	3400	1200	1480	1375	1050	110	200	10 – 2000
Connate Water Sat. (%)	19 – 23	13	10	15	5.64	11	20	N/A	22
WF Residual Oil Sat. (%)	26	35	22	20	35	N/A	35	N/A	N/A
GI Residual Oil Sat. (%)	8	12	1.9	N/A	24.5	5	10	N/A	N/A
Reservoir Temperature (°F)	205 – 195	168	225	164	167	218	151	226	N/A
Bed Dip Angle (Degrees)	23 – 35	8	26	36	Reef	Reef	Reef	Reef	5 – 12
Pay Thickness (ft)	31 – 30	230	186	35	648	292	824	950	15 – 25 (m)
Oil API Gravity	33	25	32.7	36	38	45	43.5	40	31 – 34
Oil Viscosity (cP)	0.9	3.7	0.45	0.667	N/A	0.19	0.43	0.46	0.6 – 1.0
Bubble Pt Pressure (psi)	3295	1985	6013	N/A	2154	3966	1375	2224	2800– 3200
GOR (SCF/STB)	500	900	1386	584	567	1800	450	509	2000
Oil FVF at Bubble Pt	1.285	1.225	1.62	1.283	1.313	2.45	1.284	1.315	1.1 – 1.4
Injection Gas	Air	N_2	CO_2	CO_2	HC	HC	CO_2	HC	HC
Minimum Miscibility Pressure (psi)	--	--	N/A	3334	2131	4640	1900	4257	--
WF recovery (% OOIP)	60	60	60 - 70	N/A	N/A	N/A	N/A	N/A	58
Oil Recovery: (%OOIP)	90.0	> 80.0	60.0	N/A	95.5	84.0	74.8	67.5	N/A

References

Backmeyer, L A, Guise, D R, MacDonell, P E, Nute, A J, "The Tertiary Extension of the Wizard Lake D-3A Pool Miscible Flood" SPE 13721, presented at the 1984 SPE 59th Annual Technical Conference and Exhibition held in Houston, Texas, September 16-19, 1984.

Bangla, V K, Yau, F, Hendricks, G R, "Reservoir performance of a Gravity stable vertical CO2 miscible flood: Wolfcamp reservoir, Wellman Unit", SPE 22898, presented at the 66th annual technical conference and exhibition of the Society of Petroleum Engineers, held in Dallas, TX, Oct 6-9, 1991.

Barkve, T, Firoozabadi, A, "Analysis of reinfiltration in fractured porous media" SPE 24900, presented at SPE 67th Annual Technical Conference and Exhibition, held in Washington, DC, Oct 4-7, 1992

Brigham, W E, "Mixing Equations in Short Laboratory Cores", SPE Journal, Feb 1974, pp. 91 – 99, Trans AMIE v. 257.

Butler, R M, "Gravity Drainage to Horizontal Wells", JCPT – 92 – 04 – 02, presented at the 42nd Annual Technical Meeting, of the petroleum society, Apr 1992, vol. 31, No. 4.

Cardenas, R L, Alston, R B, Nute, A J, Kokolis, G P, "Laboratory Design of a Gravity Stable, Miscible CO2 Process," SPE 10270, presented at the 56th Annual Fall Technical Conference and Exhibition of the SPE of AIME, held in San Antonio, TX, October 5-7, 1981.

Carlson, L O, "Performance of Hawkins Field Unit Under Gas Drive-Pressure Maintenance Operations and Development of an Enhanced Oil Recovery Project," SPE 17324, presented at the SPE/DOE Enhanced Oil Recovery Symposium held in Tulsa, Oklahoma, April 17-20, 1988.

Chalier, G, Giry, V, Madaoui, K, Sakthikumar, S, Maquignon, P H, "Three Phase Oil Relative Permeability Determination As A Key Point In The Evaluation Of A Tertiary Gas Gravity Drainage Project", SPE 30761, presented at the SPE Annual technical conference and exhibition of the Society of Petroleum Engineers, held in Dallas, TX, Oct 22-25, 1995.

Chang Y B, Coats B K, Nolen J S, “A Compositional Model for CO2 Floods Including CO2 Solubility in Water”, SPE 35164, Presented at the 1996 Permian Basin Oil and Gas Recovery Conference, Midland, Texas, 27-29 Mar1996.

Chatzis, I, Kantzas, A, Dullien, F A L, “On the investigation of gravity assisted inert gas injection using micromodels, long Berea cores and computer assisted tomography”, SPE 18284, presented at the 63rd annual technical conference and exhibition of the Society of Petroleum Engineers, held in Houston, TX, Oct, 2-5, 1988.

Christensen, J R, Stenby, E H, Skauge, A, “Review of the WAG field experience”, SPE 39883, presented at the 1998 SPE International petroleum conference and exhibition of Mexico, Villhermosa, March 3-5, 1998.

Crawford H R, Neill G H, Bucy B J, Crawford P B, “Carbon Dioxide A Multipurpose Additive for Effective Well Stimulation”, Journal of Petroleum Technology, Mar 1963, pp. 237.

Da Sle, W J, Guo, D S, “Assessment of a Vertical Hydrocarbon Miscible Flood in the Westpem Nisku D Reef,” SPE Reservoir Engineering, May 1990, pp. 147-154.

DesBrisay, C L, Ghussein, F E, Holst, P H, “Review of Miscible Flood Performance, Intisar “D” field, Socialist People’s Libyan Arab Jamahiriya,” SPE 10245, presented at the 56th Annual Fall Technical Conference and Exhibition of the Society of Petroleum Engineers of AIME, held in San Antonio, TX, Oct 5 - 7, 1981.

Dietz, D N “A Theoretical Approach to the Problem of Encroaching and Bypassing Edge Water,” Proc., Koninklijke Nederlandsche Akad. Wetenschap, Vol. B56, 1953, pp. 83.

Dumore, J M, “Stability Considerations In Downward Miscible Displacements”, SPE Journal, Dec 1964, pp. 356 – 362, Trans AMIE 231.

Durandeau, M, El-Emam, M, Anis, A H, “Successful Field Evaluation Of The Efficiency Of A Gas Gravity Drainage Process By Applying Recent Developments In Sponge Coring Technique In A Major Oil Field”, SPE 29809, presented at the SPE Middle East show held in Bahrain, Mar 11-14, 1995.

Ekrann, S, “An Analysis of Gravity-Segregated Piston-Like Displacement in Stratified Reservoirs,” SPE Reservoir Engineering, Feb 1992, pp. 143-148.

Espie, A A, Brown, C E, Narayanan, K R, Wilcox, T C, "A Laboratory investigation of gravity drainage / waterflood interaction in Prudhoe bay", SPE 28614, presented at the 69th annual technical conference and exhibition of the Society of Petroleum Engineers, held in New Orleans, LA, Oct 6-9, 1994

Fong, D K, Laflamme, A, Grenon, J P, Weaver, R, McIntyre, F, Stetski, S, "Design and Implementation of a Successful Vertical Tertiary Hydrocarbon Miscible Flood," presented at the 1999 CSPG and Petroleum Society Joint Convention, Digging Deeper, Finding a better bottom line, in Calgary, Alberta, Canada, June 14-18, 1999.

Green, D W, Willhite, G P, "Enhanced oil recovery", SPE Textbook series, Volume 6, 1998.

Gunawan, S, Caie, D, "Handil Field: Three years of lean gas injection into water flooded reservoirs", SPE 57289, presented at the 1999 SPE Asia Pacific Improved Oil Recovery Conference held in Kuala Lumpur, Malaysia, Oct 25-26, 1999.

Hill, S, "Channeling in Packed Columns", Chemical Engineering Science, no. 6 - 1, 1952, pp. 247-253.

Hinderaker, L, Utseth, R H, Hustad, OS, Kvanvik, B A, Paulsen, J E, "RUTH – A comprehensive Norwegian R&D program on IOR", SPE 36844, Presented at the SPE European Petroleum Conference held in Milan, Italy, Oct 22-24, 1996.

Holm LW, "CO2 Slug and Carbonated Water Oil Recovery Processes", Producers Monthly, Sept 6, 1963.

Howes, B J, "Enhanced oil recovery in Canada: Success in progress", Journal of Canadian Petroleum Technology, November – December 80-88, 1988.

Hsu, H H, "Numerical Simulation of Gravity-Stable Hydrocarbon Solvent Flood, Wizard Lake D-3A Pool, Alberta, Canada," SPE 17620, presented at the SPE international Meeting on Petroleum Engineering, held in Tianjin, China, November 1-4, 1988.

Jarrell P M, Fox C E, Stein M H, Webb S L, "Practical Aspects of CO2 Flooding", SPE Monograph, 2002 pp. 220.

Jayasekera, A J, Goodyear, S G, "Improved hydrocarbon recovery in the United Kingdom continental shelf: past, present and future", SPE 75171, Presented at the

SPE/DOE Thirteenth Symposium on Improved Oil Recovery held in Tulsa, OK, Apr 13–17, 2002.

Johnson W E, Macfarlane R M, Breston J N, "Changes in Physical Properties of Bradford Crude Oil When Contacted with CO2 and Carbonated Water", Producers Monthly, Nov 16, 1952.

Johnston, J R, "Weeks Island Gravity Stable CO2 Pilot," SPE 17351 presented at the SPE/DOE Enhanced Oil Recovery Symposium held in Tulsa, Oklahoma, Aril 17-20, 1988.

Kalaydjian, F, Vizika, O, Moulu, J C, "Role of wettability and spreading on gas injection processes under secondary conditions", presented at the 7th European IOR symposium, held in Moscow, Russia, Oct 27-29, 1993.

Kantzas A, Chatzis, I, Dullien, F A L, "Mechanisms of capillary displacement of residual oil by gravity assisted inert gas injection", SPE 17506, presented at presented at SPE rocky mountain regional meeting held in Casper, Wyoming, May 11-13, 1988.

Karim, F, Berzins, T V, Schenewerk, P A, Bassiouni, Z A, Wolcott, J M, "Light oil recovery from cyclic injection: Influence of drive gas, injection rate and reservoir dip, SPE 24336, presented at SPE rocky mountain regional meeting held in Casper, Wyoming, May 18-21, 1992.

King R L, Lee, W J, "An engineering study of the Hawkins (Woodbine) field", SPE 5528, SPE Journal of Petroleum Technology, Feb 1976, pp. 123 – 128.

Kulkarni, Madhav M, "Immiscible and Miscible Gas-Oil Displacements In Porous Media", MS Thesis, The Craft and Hawkins Department Of Petroleum Engineering, Louisiana State University and A & M College, Baton Rouge, LA, Jul 2003. URL: http://etd.lsu.edu:8085/docs/available/etd-0709103-175151/

Langenberg, M A, Henry, D M, Chlebana, M R, "Performance and Expansion Plans for the Double-Displacement Process in the Hawkins Field Unit," SPE Reservoir Engineering, Nov 1995, pp. 301-308.

Lepski, B, Bassiouni, Z A, "Screening of oil reservoirs for gravity assisted gas injection", SPE 39659, presented at 1998 SPE/DOE Improved Oil Recovery Symposium held in Tulsa, OK, April 19-22,1998.

Longeron, D G, Kalaydjian, F, Bardon, C, Desremaux, L M, “Gas/oil capillary pressure: Measurements and reservoir conditions and effect on gas-gravity drainage”, SPE 28612, presented at the SPE Annual technical conference and exhibition of the Society of Petroleum Engineers, held in New Orleans, LA, Sept 25-28, 1994.

Martin J W, “Additional Oil Production Through Flooding with Carbonated Water”, Producers Monthly, Jul 18, 1951.

Meszaros, G, Chakma, A, Zha, K N, Islam, M R, “Scaled model studies and numerical simulation of inert gas injection with horizontal wells”, SPE 20529, presented at the 65th SPE annual technical conference and exhibition, held in New Orleans, LA, Sept 23-26, 1990.

Moissis, D E, Miller, C A, Wheeler, M F, “A parametric study of viscous fingering in miscible displacement by numerical simulation”, Technical report 87-18, Rice University, Houston TX, June 1987, Available: Numerical Simulation in Oil Recovery, Minneapolis, Minn., 1986, pp. 227-247, Springer, New York, 1988.

Moritis, G, “Impact of production and development RD&D ranked”, Production Editor, Oil and Gas Journal, Oct 30, 1995.Vol 93, Issue 44.

Mungan, N, “An evaluation of carbon dioxide flooding”, SPE 21762, presented at the SPE Western regional meeting held in Long Beach, CA, March 20-22, 1991.

Nute, A J, “Design and evaluation of a gravity stable, miscible CO2 solvent flood, Bay St. Elaine field”, SPE 11506, presented at the Middle East Oil technical conference of the Society of Petroleum Engineers, held in Manama, Bahrain, March 14-17, 1983.

Oil and Gas Journal, Biannual EOR surveys, 1992 - 2002.

Oren, P E, Billiotte, J, Pinczewski, W V, “Mobilization of waterflood residual oil by gas injection for water wet conditions”, SPE 20185, SPE Formation Evaluation, March 1992, pp. 70-78.

Perkins, T K, Johnston O C, “A Review Of Diffusion And Dispersion In Porous Media”, SPE Journal, Mar 1963, pp. 70 – 84, Trans AMIE v. 228.

Rao, D N, “Gas Injection EOR – A New Meaning in the New Millennium,” JCPT (Feb. 2001) pp. 11-18.

Rao, D N, “Rutherford Stability Criterion”, Louisiana State University, Baton Rouge, LA.

Rao, D N, Xu, Q, Ayirala, S, Kulkarni, M, “Development And Optimization Of Gas-Assisted Gravity Drainage (GAGD) Process For Improved Light Oil Recovery” Quarterly Technical Progress Report, Jul 2003

Ren, W, Cunha, L B, Bentsen, R, “Numerical simulation and screening of oil reservoirs for gravity assisted tertiary gas injection processes”, SPE 81006, presented at the SPE Latin American and Caribbean petroleum engineering conference held in Trinidad, West Indies, Apr 27-30, 2003.

Slobod, R L, Howlett, W E, “The effects of gravity segregation in studies of miscible displacement in vertical unconsolidated porous media”, SPE Journal, March 1964, pp. 1-8.

Supraniowicz, R, Butler, R M, “Vertical confined water drive to horizontal well: Part I: Water and oil of equal densities”, Paper # 2, presented at the third technical meeting of the south Saskatchewan section, the petroleum society of CIM, held in Regina, Sept 25 – 27, 1989.

Thomas, J, Berzins, T V, Monger, T G, Bassiouni, Z A, “Light oil recovery from cyclic CO2 injection: Influence of gravity segregation and remaining oil”, SPE 20531, presented at the 65th Annual technical conference and exhibition of the Society of Petroleum Engineers, held in New Orleans, LA, Sept 23-26, 1990.

Tiffin, D L, Kremesec, V J, “A mechanistic study of gravity-assisted flooding”, SPE/DOE 14895, presented at the SPE/DOE fifth symposium on Enhanced oil recovery of the Society of Petroleum Engineers and the Department of Energy, held in Tulsa, OK, April 20-23, 1986.

Virnovsky, G A, Helset, H M, Skjaveland, S M, “Stability of Displacement Fronts in WAG Operations,” SPE Journal, Dec 1996, pp. 383-394.